Dendrimer Templated Silica Networks: Synthesis, Characterization and Application in Silver Nanoparticle Construction

Xiaojun Liu

Department of Chemistry
McGill University, Montreal, Quebec, Canada

January 2008

A thesis submitted to McGill University in partial fulfillment of the requirement of the degree of Master of Science in Chemistry

Acknowledgements

First, I would like to deeply thank my supervisor, Dr. Ashok K. Kakkar. I feel extremely fortunate to spend my graduate study period under his mentorship, guidance, and encouragement. His optimism and patience always helped me surpass the difficulties I was facing.

I am lucky to have worked with genuinely kind and motivated people from my group. I would like to thank my present colleagues, Florence Quist, Rami Hourani, Tatiana Vassilieff, and Amy Sutton for their scientific assistance as well as daily camaraderie. I would also like to thank colleagues of the past: Jessica McDonald, Samuel Mitton, Morgane Pasco and Nelly von Aderkas. I also thank Alex Adam Czerniewski, Olivier Rolland, and Mickael Four for their contributions on previous research work.

I gratefully acknowledge the assistance provided by the following contributors:

Mr. Fred Morin for his help with the NMR measurements,
Mr. Robert Gagnon for his help with the XRPD spectra,
Ms. Jennize Mui for her help with the TEM measurements.

An appreciation also goes out to the entire Chemistry staff.

This M.Sc thesis could not have been achieved without the support and encouragement of my parents, my brothers and sisters, and my parents-in-law, physically far away but always present when I needed them. Finally, my heartfelt gratitude goes to my wife, Yue Sun, for her tremendous love and sacrifice over the past years, and my special thanks go to my beloved new baby daughter, Amanda, for keeping me energized with her cute smile and innocent, funny actions.

Abstract

In this thesis, 3,5-Dihydroxybenzylalcohol (DHBA) based dendrimers of generations 0-5 (G0-G5) were used as templates in the construction of hybrid silica networks via a simple sol-gel condensation methodology. Two types silane reagent $Si(NMe_2)_4$ and $ClSi(NEt_2)_3$ were used to react with the periphery situated hydroxyl groups in these dendrimers, followed by hydrolysis and polycondensation, leading to highly cross-linked, porous silica based hybrid materials. The removal of dendrimer templates was achieved via *in situ* or acid hydrolysis. *In situ* removal of dendrimer templates was carried out as the use of $ClSi(NEt_2)_3$, while in the case of $Si(NMe_2)_4$, the dendrimers were subsequently removed upon treatment with HCl. The detailed studies of silica network structures and surface morphology before and after removal of dendrimers and salt were carried out using techniques including solid-state NMR, FT-IR spectroscopies, transmission electron microscopy (TEM), and nitrogen adsorption (BET), showing that the aggregation of DHBA based dendrimers controls the evolution of the network structure and their pore sizes. The resulting dendrimer templated silica networks were found to be water repellant on their surfaces with a hydrophilic interior.

The application of silica networks synthesized using DHBA based dendrimers as templates was successfully demonstrated in tailoring the preparation of silver metal nanoparticles. Due to the internal and external environment of the silica networks, G1-3 silica networks wet slowly with aqueous silver acetate, resulting in chemisorption of silver ions with internal silanol groups, and followed by the growth of silver oxide nanoparticles as higher local water content around silver ions inside the networks. G4 silica networks with residual of dendrimer templates mixed with aqueous silver acetate solution. Silver ions that were chemisorbed with silanol groups were reduced photolytically to silver metal under a stabilizing dendrimer environment, leading to the formation of silver metal nanoparticles exclusively.

Résumé

Au cours de ce master, des réseaux hybrides de silice ont été synthétisés par simple condensation sol-gel et à l'aide de dendrimères de générations 0 à 5 (G0-G5), dont le squelette a été formé à partir de l'alcool 3,5-dihydroxybenzylique. Deux types de réactifs, $Si(NMe_2)_4$ et $ClSi(NEt_2)_3$, ont été employés de manière à réagir avec les groupements hydroxyles terminaux de ces dendrimères. Puis, par hydrolyse et polycondensation, des réseaux de silice très réticulés et poreux ont pu être produits. La suppression des dendrimères a été réalisée *in situ* ou par hydrolyse acide.En effet, l'élimination des dendrimères a lieu dans le cas du réactif $ClSi(NEt_2)_3$, tandis qu'avec $Si(NMe_2)_4$, un traitement avec l'acide chlorhydrique HCl a été nécessaire. Une étude détaillée des réseaux de silice, c'est-à-dire leur morphologie avant et après l'élimination des dendrimères et les sels, a été menée en utilisant diverses techniques telles que la RMN à l'état solide, la spectroscopie FT-IR, la microscopie électronique à transmission (TEM) et la technique d'adsorption d'azote (BET). Les résultats de la technique BET ont par ailleurs montré que l'agrégation des dendrimères précédant la synthèse sol-gel contrôle l'évolution de la structure du réseau et la taille de leurs pores. De plus, ces réseaux de silice ont été observés comme rejetant les molécules d'eau à leur surface et étant constitué d'un intérieur hydrophile.

Enfin, il a été démontré avec succès que ces réseaux de silice pouvaient être appliqués à la préparation de nanoparticules d'argent. Dû à leur environnement hydrophobe, les réseaux de silice G1-3 réagissent très lentement avec l'acétate d'argent aqueux, engendrant la chimisorption des ions argent à l'intérieur hydrophile des réseaux. Localement, les molécules d'eau se trouvent en quantité plus importante autour des ions argent permettant ainsi la formation et la croissance des nanoparticules d'argent à l'intérieur des réseaux. En ce qui concerne les réseaux de silice G4, contenant des dendrimères résiduels, ils réagissent vite avec l'acétate d'argent contenu en solution aqueuse. Ensuite, les ions argent qui sont chimisorbés à l'intérieur de ces réseaux sont réduits par photolyse en métal d'argent dans un environnement stabilisant qu'est celui des dendrimères. Ceci conduit exclusivement à la formation de nanoparticules d'argent.

Table of Contents

List of Figures

List of Schemes

List of Tables

Abbreviations

BCC	Body-centered cubic
BET	Brunauer-Emmett-Teller
Brij76	Polyethylene glycol octadecyl ether
cac	Critical aggregation concentration
cmc	Critical micelle concentration
CYL	cylindrical micelles
DHBA	3,5-dihydroxybenzyl alcohol
DMF	*N,N*-dimethyl formamide
DR1	Disperse red 1
DSC	Differential Scanning Calorimetry
EO-PO-EO	Polyoxyethylene –polyoxypropylene –polyoxyethylene
FT-IR	Fourier transform infrared
G_n	Generation number
HEX	Hexagonally ordered cylinders
HPL	Hexagonally pinhole layers
LAM	Lamellae
LCT	Liquid-crystal templating
MIC	Spherical micelles
MLAM	Modulated lamellae
NMR	Nuclear magnetic resonance
OS	Organosilicons
PAMAM	Poly(amido amine)
PEO	Poly(ethylene oxide)
PEO_n-PPO_m-PEO_n	Poly(ethylene oxide)-poly(propylene oxide)-poly(ethylene oxide)
PPI	Poly(propylene imine)
PVP	Poly(vinyl pyrrolidone)
SEM	Scanning electron microscopy
SERS	Surface-enhanced Raman scattering
TEM	Transmission electron microscopy

TEOS	Tetraethyl orthosilicate
TGA	Thermal Gravimetric Analysis
THF	Tetrahydrofuran
TMOS	Tetramethyl orthosilicate
UV-Vis	Ultra violet-visible
XPD	X-ray diffraction
XRPD	X-ray powder diffraction

Chapter 1: Introduction to Silica Based Networks

Silicon is the second most abundant element in the earth’s crust [1]. In nature silicon combines with oxygen and forms a multitude of silicate minerals. Despite the intensive studies on silicon dioxide (silica) over years, it is still attracting much research interest in different fields [2]. A great number of natural materials, which possess cavities, cages, or tunnels, such as zeolites [3], are not only of high academic interest but also of intense practical value because they exhibit well-defined host-guest chemistry [4]. Among these porous solids, silica based networks, with tailor-made pore sizes and shapes, exhibit a distinguished importance, being the most studied systems in which many applications such as drying agents, adsorbents, and storage systems [5] could be carried out based on molecular recognition. Silica based networks present a great variety of possible structures because of the flexibility of tetracoordinated Si, and easy control of the sol-gel process (hydrolysis and condensation reactions). Much effort was devoted to creating these zeolite-like materials, and led to the discovery of the first novel mesoporous silica networks of M41S family, such as MCM-41, which were obtained by Mobil in 1992 [6]. Soon after this discovery, significant research effort has been extended to achieve control over physical characteristics of mesoporous silica, including pore size and morphology, by incorporating a broad range of organic and inorganic materials as templates. These templates may be defined as a central structure around which a silica network develops in such a way that removal of the template creates a cavity with morphological features related to those of the template [7]. These morphological features could be affected by the association of the template with silica matrix, such as interactions between template and silica matrix, and the relative size of template used to construct the silica matrix.

1.1 Sol-Gel Process

In sol-gel chemistry, the term “sol” means the suspension of colloidal particles in solution. These colloidal particles are nanometer-sized solid particles and could interconnect with one another in three dimensions to form a gel, the rigid network with pores and polymeric chains [8]. The sol-gel process generally starts with alcoholic solution of monomeric, metal or semimetal alkoxide precursors such as tetraethyl orthosilicate (TEOS, $Si(OEt)_4$). This reaction is divided into two steps: hydrolysis of alkoxide precursors to form hydroxyl groups, followed by polycondensation of the hydroxyl groups to form a three-dimensional network (gel). The hydrolysis step involves mixing of alkoxide precursor, such as $Si(OR)_4$, where R is CH_3, C_2H_5, or C_3H_7, with water.

Hydrolysis:

$$Si(OCH_3)_4 + 4\,H_2O \longrightarrow Si(OH)_4 + 4\,CH_3OH$$

Scheme 1. 1. Hydrolysis of tetramethylorthosilicate (TMOS).

Si-O-Si bonds are formed by the condensation of the resulting silanol $Si(OH)_4$. The continuation of this condensation process (polycondensation) results in three-dimensional silica particles.

Condensation:

$$2\,Si(OH)_4 \longrightarrow (OH)_3Si\text{-}O\text{-}Si(OH)_3 + H_2O$$

Scheme 1. 2. Condensation of silanol to form Si-O-Si bond.

Polycondensation:

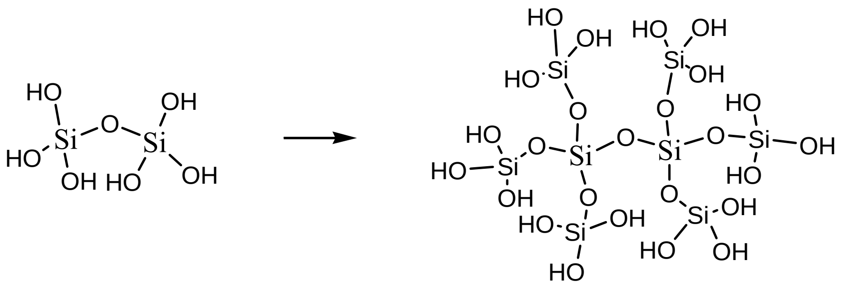

Scheme 1. 3. Polycondensation to form silica networks.

The sol is produced when sufficient interconnected Si-O-Si bonds are formed through hydrolysis and polycondensation reactions. The size of the sol particles depends on the specific experimental conditions, generally with diameters of 1-100 nm [9]. The sol can evolve in different ways according to the reactions of steps that follow. According to Brinker's study [10], an overview of the sol-gel process is shown below (Figure 1.1).

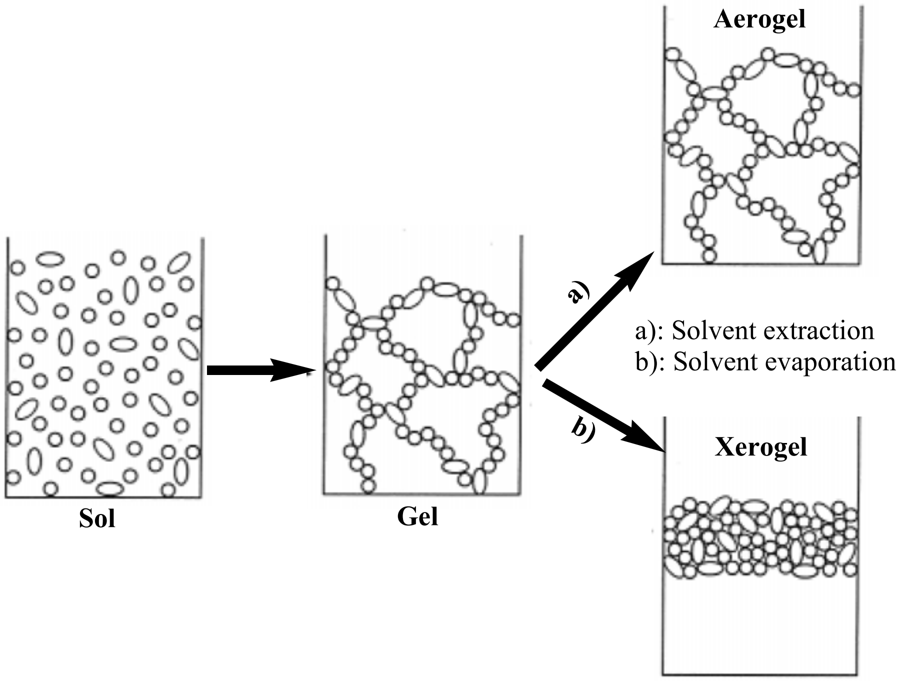

Figure 1. 1. Overview of the sol-gel process (adapted from [11]).

The sol colloidal is linked together to form a three dimensional, liquid-filled gel in gelation step. Different properties of materials are obtained depending on sol particle transformation to a gel, which can be initiated by several methods including gelation of a solution of colloid particles, hypercritical drying, or aging and drying under ambient atmosphere. These methods affect the structural properties of gels by the removal of solvent, solvent extraction (hypercritical drying) preserves the original 3D structure and produces low density networks (termed *aerogel*, which can have pore volumes 98% and densities as low as 80 kg/m^3 [12, 13]), while solvent evaporation (drying under ambient atmosphere) results in the structural collapse of networks, creating a higher density monolith material (termed *xerogel*). If heated to high temperatures, this porous xerogel can form the dense ceramic. If the sol solution is coated on a solid substrate, followed by subsequent gelation and solvent evaporation, the xerogel film will be formed. Dense films are formed by heating at high temperatures.

The term *gel* usually applies to either *xerogel* or *aerogel* and is defined as *dried* when the physically adsorbed water is completely removed. This interconnected, rigid network has submicrometer pores and polymeric chains with average length greater than a micrometer. Flory [14] discussed the diversity of this combination and suggested four kinds of categories: (1) well-ordered lamellar structures; (2) covalent polymeric networks, completely disordered; (3) polymer networks formed by physical aggregation, mainly disordered; and (4) particular disordered structures.

Sol-gel process has long been used for the powderless processing of glasses and ceramics [15]. The first sol-gel processing of silica materials into ceramics and glass was studied by Ebelmen [16, 17] and Graham [12], as early as in the mid-1800s. They observed that under acidic conditions tetraethyl orthosilicate (TEOS), $Si(OC_2H_5)_4$, hydrolyzed to form glass like SiO_2 material. From then on, lots of studies were carried out to investigate the synthesis of a variety materials by sol-gel processing [8, 15]. It has been widely used in the synthesis of multicomponent and nanophase materials by controlling the structure of a material on a nanometer scale, from the earliest stages of processing, resulting in higher purity and greater homogeneity [8, 15]. Because it can be carried out at much lower temperatures than traditional methods, materials formed by this sol-gel process show attractive properties such as structures with large open spaces of porosity, controllable hydrophobicity, chemical capacity for modification or encapsulation of various components [18].

One of the major advances of sol-gel processing is undoubtedly the synthesis of organic-inorganic hybrid materials. The combined properties of organic and inorganic components in unique composite materials contributed to promising applications in many fields, from the earliest painting materials to innovative advanced materials for applications in optics, electronics, ionics, mechanics, membranes, protective coatings, catalysis, sensors, biology, and others [19]. The mild chemistry involved in the sol-gel process makes the preparation of organic-inorganic hybrids materials easily achievable, and resulting in nanocomposite materials with unique properties, which the traditional macroscale composites and conventional materials do not have. The preparation, characterization, and applications of organic/inorganic hybrid materials have rapidly become a fast expanding area of research in materials science [20]. The organic moieties can be introduced into hybrid networks through strong covalent chemical bonds or by the weak interactions such as van der Waals and hydrogen bonds. Wen [20] summarised these techniques to include more than seven kinds of synthetic strategies incorporating various starting inorganic and organics: organoalkoxysilanes as precursors to form ≡Si-C- bond [21-24]; the co-condensation of functionalized oligomers or polymers with metal alkoxides [25-27]; *in situ* formation of inorganic particles within a polymer matrix [28-30]; or organics are simply impregnated or entrapped within inorganic matrixes as guests [31, 32]. The first two methods include covalent connectivity between organic and inorganic components (Scheme 1.4). In the others, there are no covalent bonds formed between organic and inorganic components, the organics are just entrapped inside the pores of inorganic materials formed by polycondensation process. Formation of organic-silica hybrid network materials by the sol-gel process is shown in Scheme 1.4.

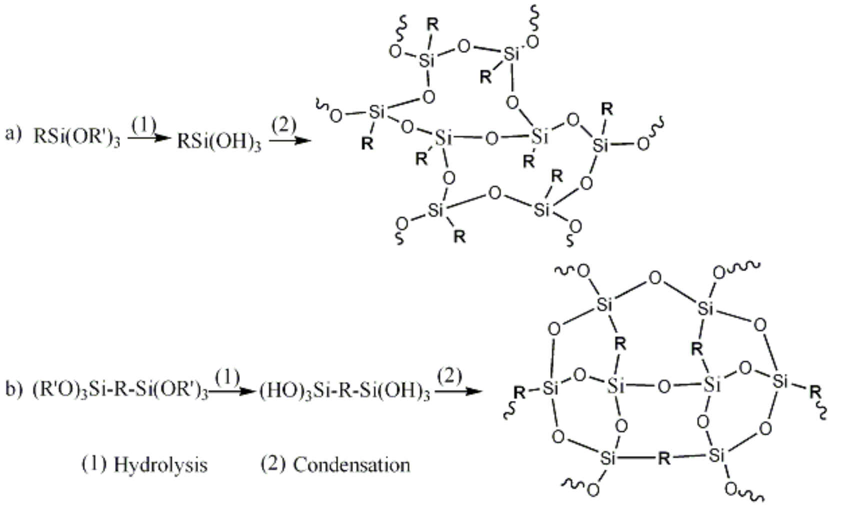

Scheme 1. 4. General synthetic methods for organic-inorganic hybrid materials by using covalent bonds.

1.2 Synthesis of Silica Networks Using Templates

In the organic-inorganic hybrid silica materials, the removal of organic components (or some inorganics) (which could be termed as *templates*) can form silica networks with porous internal environment. This organized, highly cross-linked silica network material with a desired porous internal environment and large specific surface area, aroused intense scientific interest for a variety of applications including selective catalysis, drug delivery [33, 34], adsorption [35, 36], and host-guest chemistry [37, 38]. These periodic ordered structures might be microporous (<2 nm), mesoporous (2-50 nm), or macroporous (>50 nm) [37]. Such systems that can provide complementarity in terms of size and shape between the network host and incoming guest will lead to pathways for predicting and controlling their release profile [33, 39, 40]. Numerous methods to achieve this goal have been used in the past that have employed natural (Figure 1.2) [41] or synthetic inorganic or organic templates to create pores with controlled structural features. The inorganic templates include zeolites, mesoporous molecular sieves, and silica gel [37], as well as lots of organics such as surfactants, polymers, dendrimers, and other colloidal particles [6, 42-44].

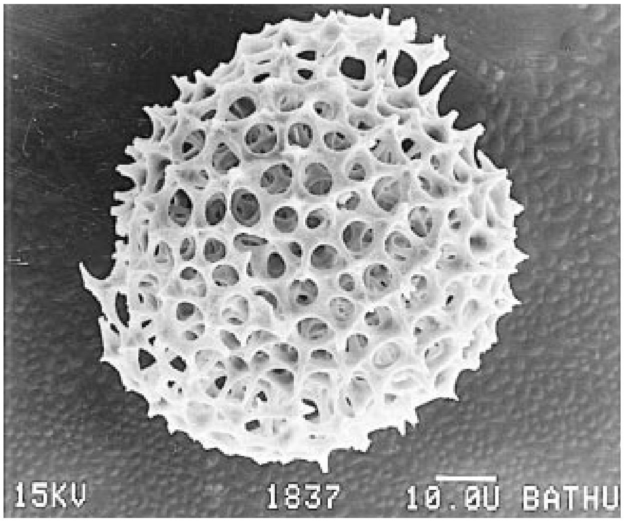

Figure 1. 2. Scanning electron micrograph of a silica microskeleton formed by biomineralization in a single-celled organism [41].

1.2.1 Surfactant-Templated Synthesis of Silica Networks

Surfactants (term comes from “surface active agent”) are bifunctional molecules that consist of a hydrophilic (water soluble) head group and a hydrophobic (water insoluble) tail. The hydrophobic tail usually consists of hydrocarbon or fluorocarbon chains, while the hydrophilic head consists of a polar group such as -OH, -COOH, $-NH_3^+$, $-PO_4(CH_2)_2NH_3^+$, etc. This amphiphilic nature of surfactants is responsible for their association behavior in solution, forming surpramolecular arrays (micelles, bilayers, vesicles, etc.) which depend on the surfactant concentration [45]: surfactants are present as free molecules in solution at very low concentration. As the concentration increases, after higher than the critical micelle concentration (*cmc*), the individual surfactant molecules form small, spherical aggregates, called micelles. Continued increase in concentration forms cylindrical micelles and then hexagonal arrays, cubic, and even lamellar phase at very high concentration (Figure 1.3). Different surfactants with a variety of sizes, shapes, and charges have been used as templates to synthesize silica networks. Based on the head group chemistry and charges, surfactants mainly include three types of molecules: anionic (negative charges in the hydrophilic head, such as $C_nH_{2n+1}OSO_3$, n=12, 14, 16, 18) [46], cationic (positive charges in the hydrophilic head, such as alkylammonium salts, $C_nH_{2n+1}(C_2H_5)_3N$, n=12, 14, 16, 18) [46], and nonionic (the hydrophilic group is not charged, including primary amines [47] $C_nH_{2n+1}NH_2$, EO-PO-EO polymers [44], etc).

The development of porous silica networks has currently attracted a lot of interest, since the studies related to using surfactants as templates were first reported in the early 1990’s by Mobil Oil [48] and Kuroda’s group [49, 50]. The number of research papers, which focus on the mesostructured silica networks, has increased tremendously during the last decade [44]. This class of periodic mesoporous silica networks are well-known as the M41S phase, including three representatives such as MCM-41, MCM-48, MCM-50 [6, 48, 51] (Figure 1.3).

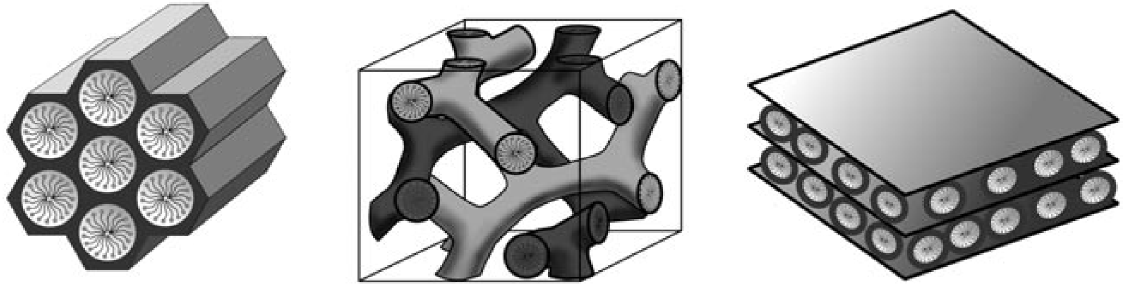

a) b) c)

Figure 1. 3. Structures of mesoporous M41S networks: a) hexagonal (MCM-41, space group p6mm), b) cubic (MCM-48, space group Ia3d), and c) lamellar (MCM-50, space group p2) [51].

The methodology to synthesize mesoporous silica networks is to employ simple organosilicate compounds, such as tetramethyl orthosilicate (TMOS) and tetraethyl orthosilicate (TEOS), as the silica precursors. The formation of mesostructured silica networks is carried out by using supramolecular aggregates of ionic surfactants as templates. These ionic surfactants are self-assembled to form ordered mesostructured composites during the condensation process, then followed by the removal of surfactants, leading to the formation of mesostructured silica networks. These kinds of materials can be controlled with regard to symmetry, pore size (pore diameters within the range of 2-10 nm), and exhibit amorphous pore wall with very large specific surface area. Figure 1.4 gives a schematic representation of this methodology [5].

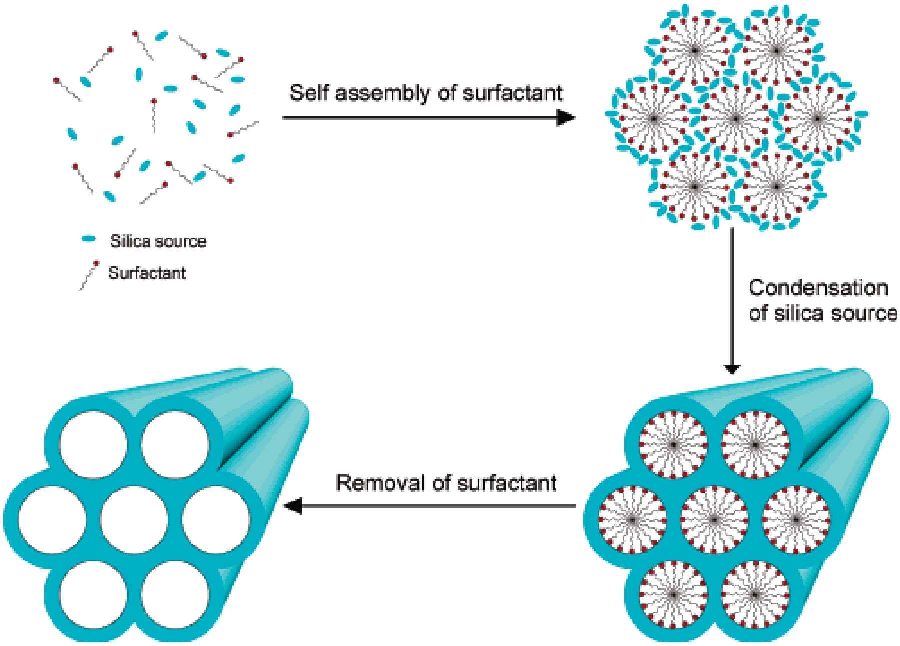

Figure 1. 4. Representative of the synthetic procedure of silica networks by using surfactants as templates [5].

Two main classes of surfactants are used as templates in the preparation of mesoporous silica networks: ionic and nonionic [3, 44, 45, 51]. The cationic surfactants are commonly used in this field. For example, $C_nH_{2n+1}(CH_3)_3N^+X^-$ cationic surfactants were employed as templates to prepare hexagonal (space group *p6m*) [52], cubic (space group *Ia3d*) [53], and lamellar (space group *p2*) mesoporous silica networks. The nonionic surfactants containing polyoxyethylene chains, such as block copolymers polyoxyethylene –polyoxypropylene -polyoxyethylene (referred to as EO-PO-EO), have also been used as templates in the preparation of mesoporous silica networks with both hexagonal and cubic geometries as well [44].

Two different mechanisms are involved in the formation process of silica networks: liquid-crystal templating (LCT) [54] and cooperative liquid-crystal templating [55]. In LCT, a lyotropic liquid-crystal is formed by self-assembly before silica precursor is added. At low concentration, the surfactant undergoes cooperative self-assembly with the silica source, developing a liquid-crystal phase with hexagonal, cubic, or laminar arrangement (Figure 1.5) [51].

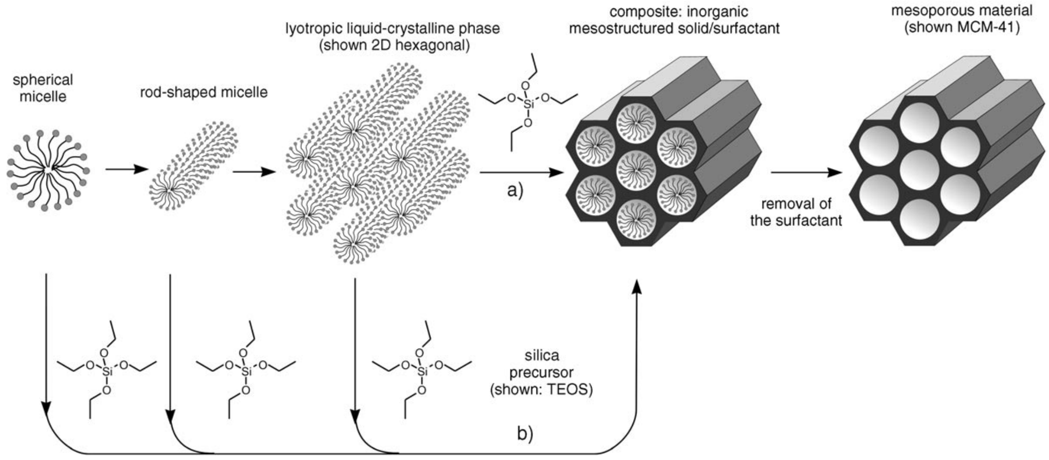

Figure 1. 5. Formation mechanisms of mesoporous silica networks: a) TLCT, b) cooperative mechanism [51].

It is important to understand the interactions between templates and silica precursors, and several mechanisms have been proposed in this regard. Huo *et al* [46, 56, 57] suggested four different routes that can explain the formation of ionic surfactant-templated mesostructures during the preparation of surfactant-templated silica networks. They are based on electrostatic interactions taking place at different pH values. The overall procedure that takes place is as follows (Figure 1.6): a) (S^+I^-) (in the basic solution, silicate anions (I^-) combine with cationic surfactant (S^+)), b) ($S^+X^-I^+$) (if pH is acidic, protonated silicate (I^+) combines with cationic surfactants (S^+) after the addition of inorganic ions X^-, such as Cl^-, Br^-); c) (S^-I^+) (in acidic condition, protonated silicate (I^+) interacts with anionic surfactants (S^-)), and d) ($S^-M^+I^-$) (in a basic solution, the addition of metal ions M^+, leads to the combination of silicate anions (I^-) with anionic surfactants (S^-)). In the case when the nonionic surfactants are used, the model of e) (S^0I^0) [47, 58] or the ion pair f) (S^0)$(IX)^0$ [59] (under acid conditions, inorganic ions X^- such as Cl^- and Br^- are needed), can be presented due to the formation of hydrogen bonds or dipolar interaction between surfactant and silica species.

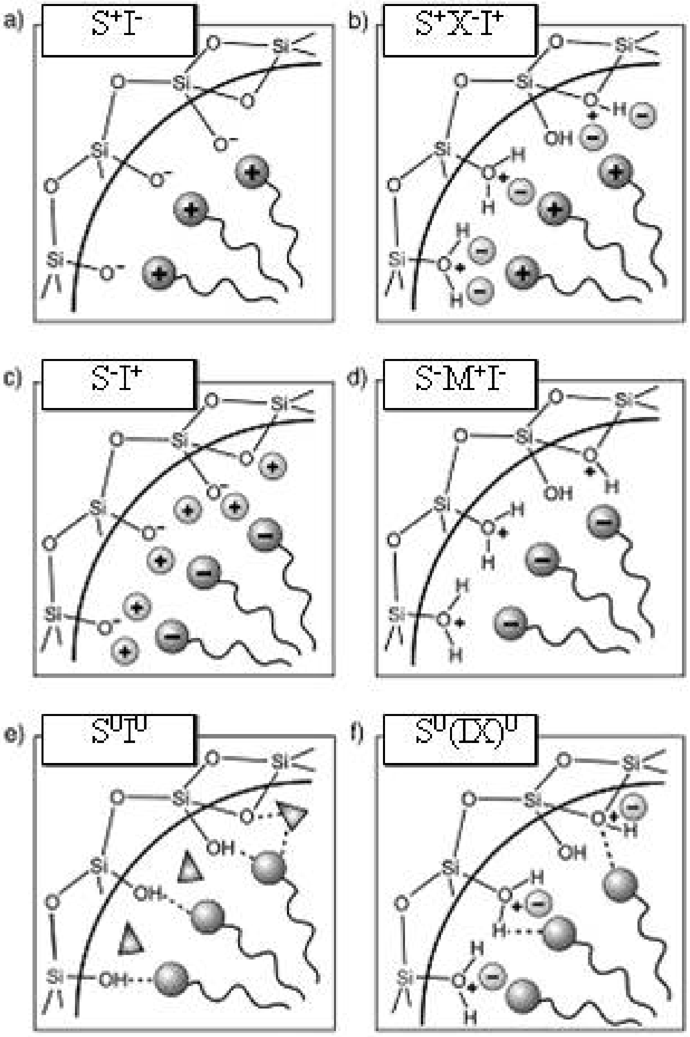

Figure 1. 6. Schematic representation of the mechanisms proposed for the formation of mesoporous silica networks using surfactants as templates [51].

1.2.2 Polymer-Templated Synthesis of Silica Networks

The synthesis of silica networks with controlled porosity can also be carried out by using polymers as templates. The subsequent removal of polymer templates results in the desired porosity in silica networks. Polymeric templates provide vast opportunities in the pore size and pore structure tailoring of silica networks, leading to fibers, continuous films, rods, mesoporous-macroporous membranes, monoliths, spheres, etc [60]. Amphiphilic block copolymers are excellent templates in building the structure of silica networks, as well as diblock or triblock coplymers [3]. The varied morphologies of amphiphilic block copolymers gives different structures such as body-centered cubic (BCC), hexagonally ordered cylinders (HEX), gyroid (Ia3d), hexagonally pinhole layers (HPL), modulated lamellae (MLAM), lamellae (LAM), cylindrical micelles (CYL), and spherical micelles (MIC)(Figure 1.7) [61].

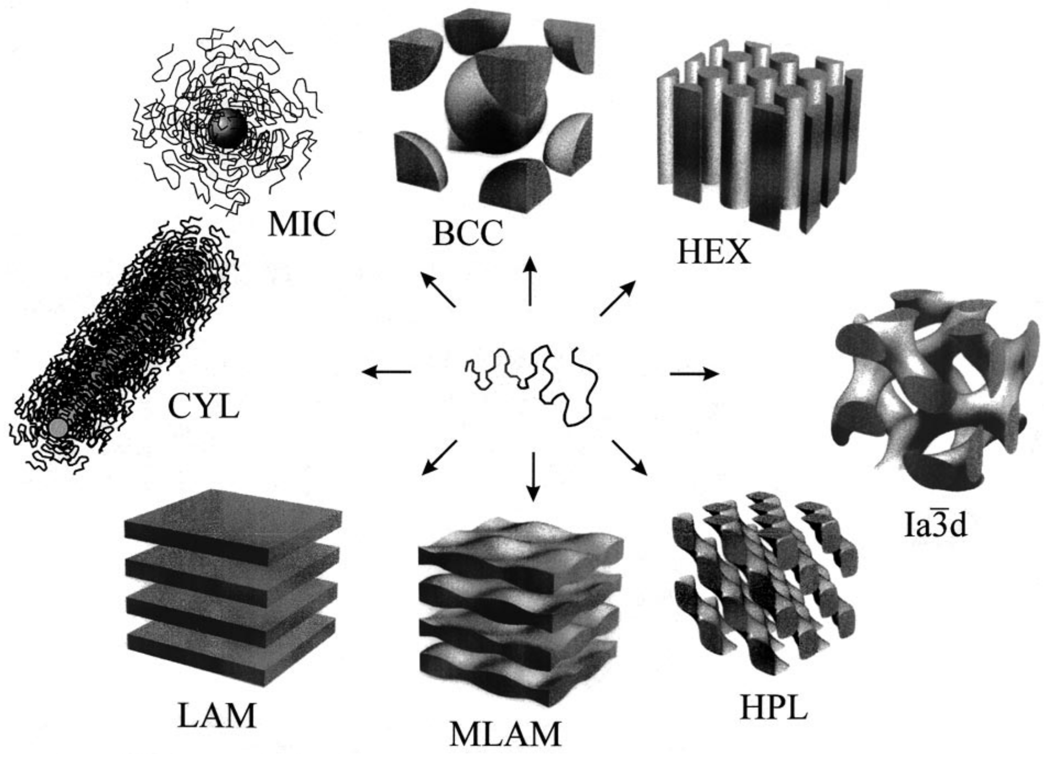

Figure 1. 7. Main morphologies of amphiphilic block copolymers [61].

The remarkable contribution to polymer-templated silica networks has been made by Stucky and co-workers [62], who synthesized highly ordered mesoporous silica network using commercially available nonionic alkyl poly(ethylene oxide) (PEO) and poly(alkylene oxide) block copolymers as templates. In the presence of PEO_n-PPO_m-PEO_n (poly(ethylene oxide)-poly(propylene oxide)-poly(ethylene oxide)), the cubic (such as SBA-11,16 [63]), 3D (such as SBA-12) or 2D hexagonal (such as SBA-15 [60, 64]), and lamellar mesoporous silica structures can be prepared. Large EO segments promote the formation of lamellar silica networks, while low EO segments favor cubic silica structures. The subsequent studies related to triblock-copolymer templating was followed by many other groups [63-65], and led to more mild reaction conditions such as moderately acidic or acid-free condition. Other kinds of polymers were also employed as templates in the synthesis of mesoporous silica networks [66-68].

1.2.3 Dendrimer-Templated Synthesis of Silica Networks

Dendrimers are monodisperse, highly branched, three-dimensional macromolecules with a multivalent core, as well as terminal function units at the periphery (Figure 1.8). After an iterative sequence of reactions, the successive generation of dendrimers are obtained, presenting different sizes, shapes, and terminal units of the branches which can be efficiently controlled [69-71]. Because of the well-defined structure as well as a definite number of peripheral groups, dendrimers offer numerous advantages for a variety of applications. For example, their internal cavities can be loaded with guest molecules for drug delivery purposes [72-74]. Functionalization of the periphery or the internal backbone with transition metals can result in highly efficient and easily recoverable catalysts [75, 76]. Incorporated dendrimers within silica can allow production of supported catalysts [77], chromatographic supports [78], or porous membranes [79].

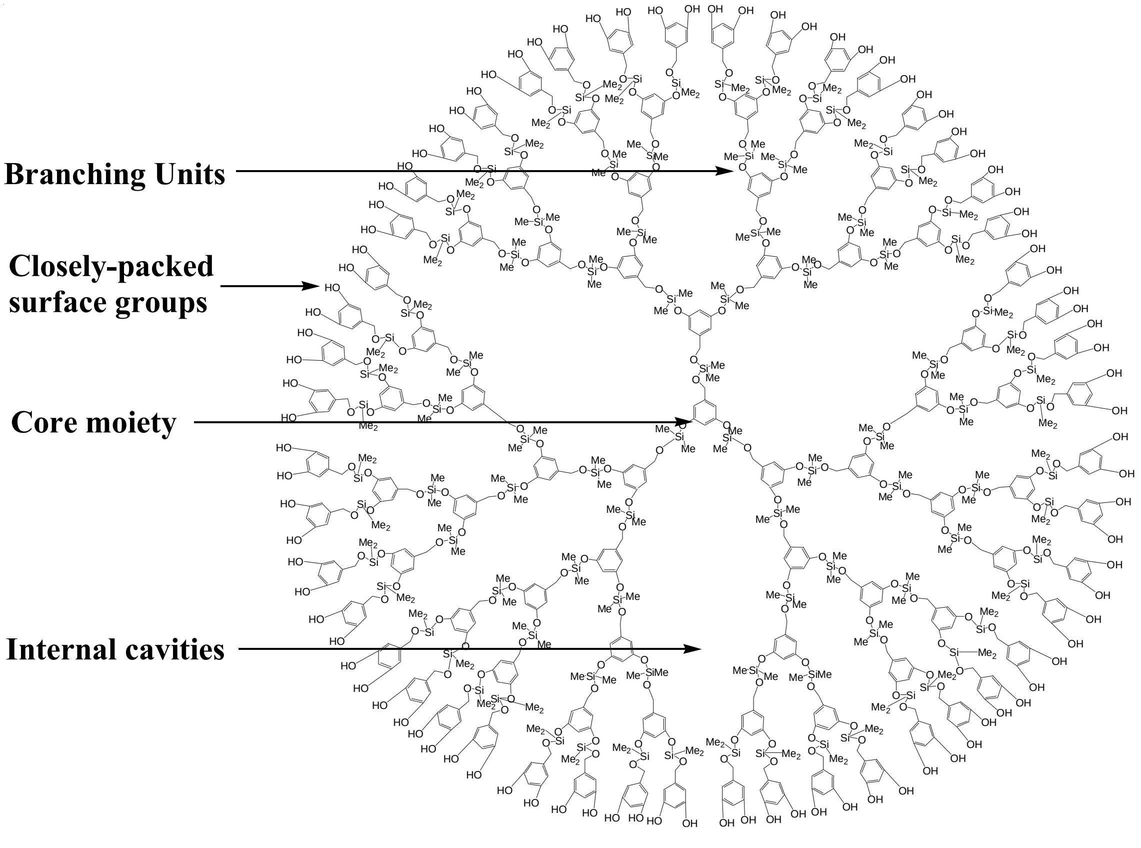

Figure 1. 8. Representative dendrimer structure [80].

Due to the unique architecture of a dendrimer there are many possibilities for size and shape control of the final organic-inorganic hybrid materials. The applications of dendrimers are expanded now to the fields of sol-gel synthesis of network materials, such as micro- and mesoporous silica networks [81-84] and nanomaterials [84-86]. Dendrimers are employed as organic templates to form hybrid nanomaterials with specific properties. The removal of these dendrimer templates could lead to the formation of nanoporous silica networks with specific nanoporous cavities, which are dependent on the individual dendrimer's specific architecture and the reaction conditions, with the pore size range from few to hundred nanometers.

A variety of dendrimers has been employed as organic templates in the synthesis of nanoporous materials [84, 87-93]. Among hybrid organic-inorganic materials, dendrimer based xerogels have potential applications as catalysts, supports, and porous membranes [90]. Carbosilane dendrimers were first used to prepare hybrid organic-inorganic networks by Michalcayk and co-workers [92]. They designed and synthesized different types of dendrimer, which comprise a number of flexible radial arms terminating in trialkoxysilane groups with an atomic, linear or cyclic core (the first generation dendrimers, termed star molecule) (Figure 1.9). Low surface area network materials (star gel) were formed by the hydrolysis and condensation of these terminated groups of Si(OR)$_3$, which can also co-network with tetraalkoxysilanes, in the same way as tetraalkoxysilanes do in the conventional sol-gel process. The condensation procedure can occur by inter- and intra-molecular process. The degree of condensation in these gels was measured by solid-state ^{29}Si NMR. In here the "T^n" notation for RSiO$_3$ centers replaces the conventional "Q^n" notation for SiO$_4$ tetrahedra. The terminal dendritic silicons with one, two, and three Si-O-Si linkages are designated T^1, T^2, and T^3 [94]. The results showed that more than 66% of silicon atoms were T^2, with equal amount of T^1 and fully condensed T^3.

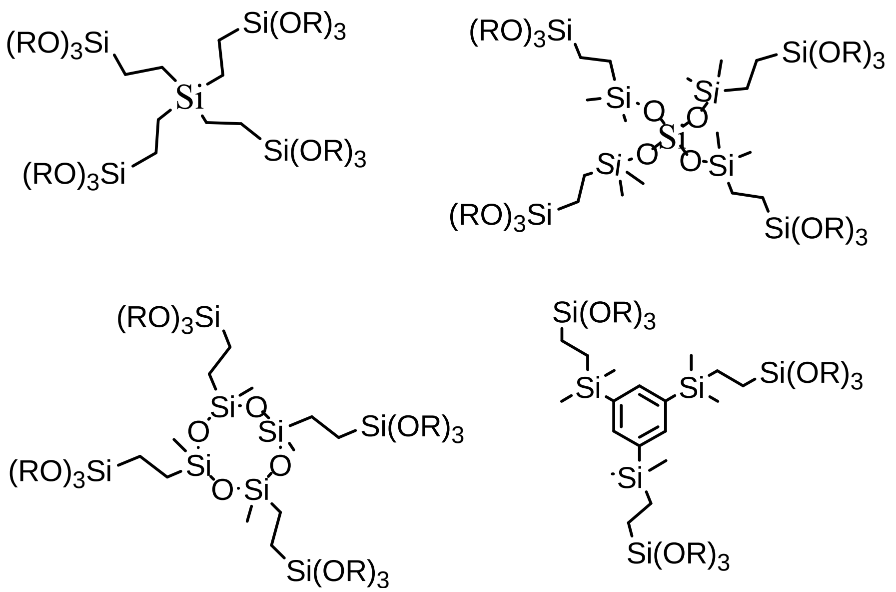

Figure 1. 9. Representative structures of star molecules, the first generation of silicon containing dendrimers [92].

The inter-molecular and intra-molecular mechanisms for the condensation reaction were also shown by Corriu and co-workers [89], who tried to use the second generation carbosilane dendrimer with trimethoxysilyl-terminated groups to make hybrid xerogels, getting a higher surface area of up to 684 m^2g^{-1}. Tilley and co-workers [90, 91] reported the synthesis of second and third generation carbosilane dendrimer-based xerogels (Figure 1.10). The relatively high surface area materials were prepared by the acid-catalyzed hydrolysis of second and third generation dendrimers with alkoxysilyl terminated groups in THF solution. The results show that the total surface area and pore volume increase with generation number (surface area: 325 m^2g^{-1} for X-G2 and 490 m^2g^{-1} for X-G3, pore volume: 0.21 ccg^{-1} for X-G2 and 0.33 ccg^{-1} for X-G3, respectively). The degree of condensation from the data of ^{29}Si NMR for both gels was approximately 68%. Further investigations, which were carried out by changing the reaction conditions, such as using nonpolar solvents or high drying temperatures, indicates that the considerable collapse could be avoided, allowing the synthesis of remarkable high surface area mesoporous, dendrimer-based materials (600-1300 m^2g^{-1}).

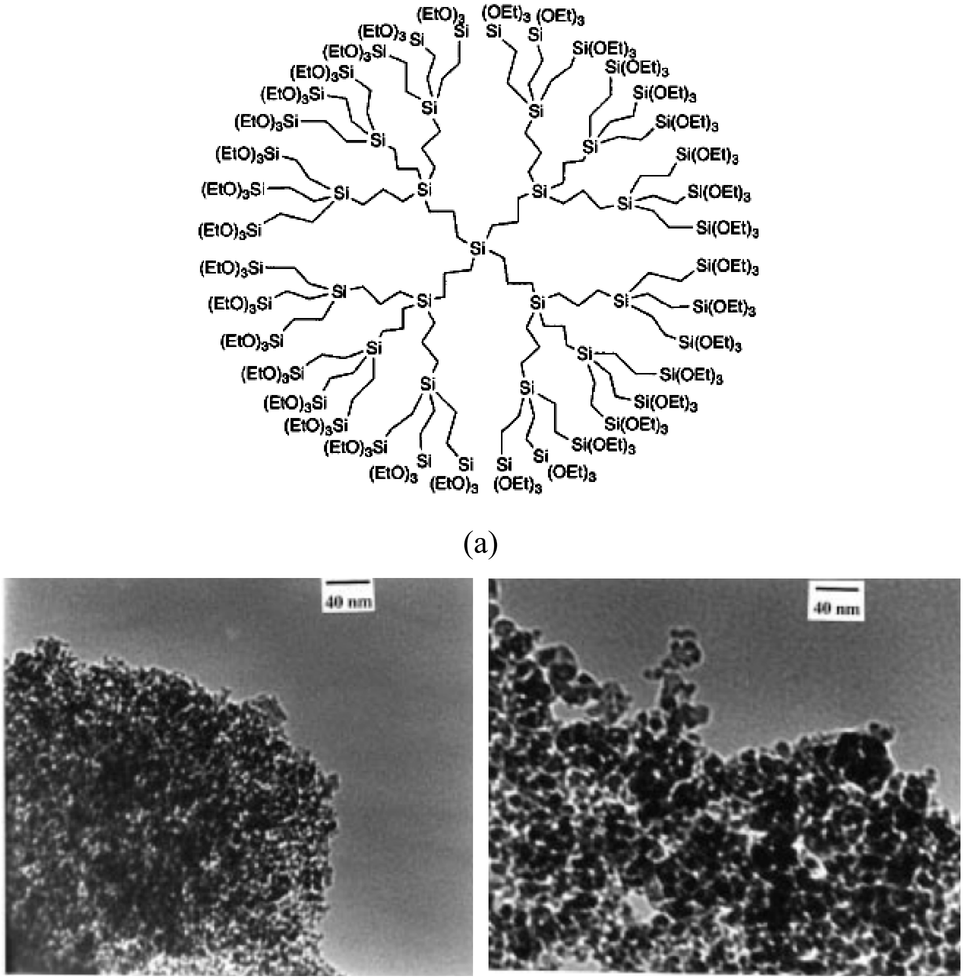

(a)

(b) (c)

Figure 1. 10. Representative of carbosilane dendrimer (a) of G3'-(OEt) $_{108}$ and the TEM images of (b) X-G2' and of (c) X-G3'[90].

Caminade and Majoral [84, 87] studied the applications of phosphorus-containing dendrimers in the field of materials science. A large amount of phosphorus dendrimers with various types of end groups, cores, and different generations were studied for constructing hybrid organic-inorganic materials. Different size of dendrons, bearing the $Si(OEt)_3$ at the core and occupying various types of end groups, were reacted with $Si(OEt)_4$ through sol-gel process. Varieties of dendron-silica xerogels were obtained by the hydrolysis and polycondensation. Some of them show mesoporosity with a narrow pore size distribution. The removal of phosphorus dendrimers from the hybrid solid by heating gives a highly porous material, which could be expected to use as absorbents or insulating materials.

The most common dendrimers which are used in the construction of nanomaterials are amine dendrimers [83, 85, 86, 95-102], such as poly(propylene imine) (PPI) and poly(amido amine) (PAMAM) dendrimers with amine-terminated groups which could contribute to dendrimer aggregation by forming hydrogen bonds. A great number of studies were carried out in the formation of these kinds of dendrimer-silica materials. Wright's group [85, 86] have studied the formation of silica-amine dendrimer nanocomposites. The self-assembly of PPI and PAMAM dendrimer templates contribute to the size control of the silica networks (Figure 1.11). The primary amine moieties act as the acid-base catalyst in which deprotonated residues (base) accept a proton from silicic acid, forming a reactive silanolate group and protonated residues (acid). The positively charged patches on the surface of the dendrimers interact electrostatically with silanolate or growing negatively charged silica species leading to silica precipitation on the dendrimer surface. The whole process is controlled through charge stablization of the growing spheres in solution. With neutralized surface formed through interactions of cations with the growing negative charges on silica surface, the electrostatic repulsion is decreased, thus, permitting the particles to agglomerate and grow to significantly larger size.

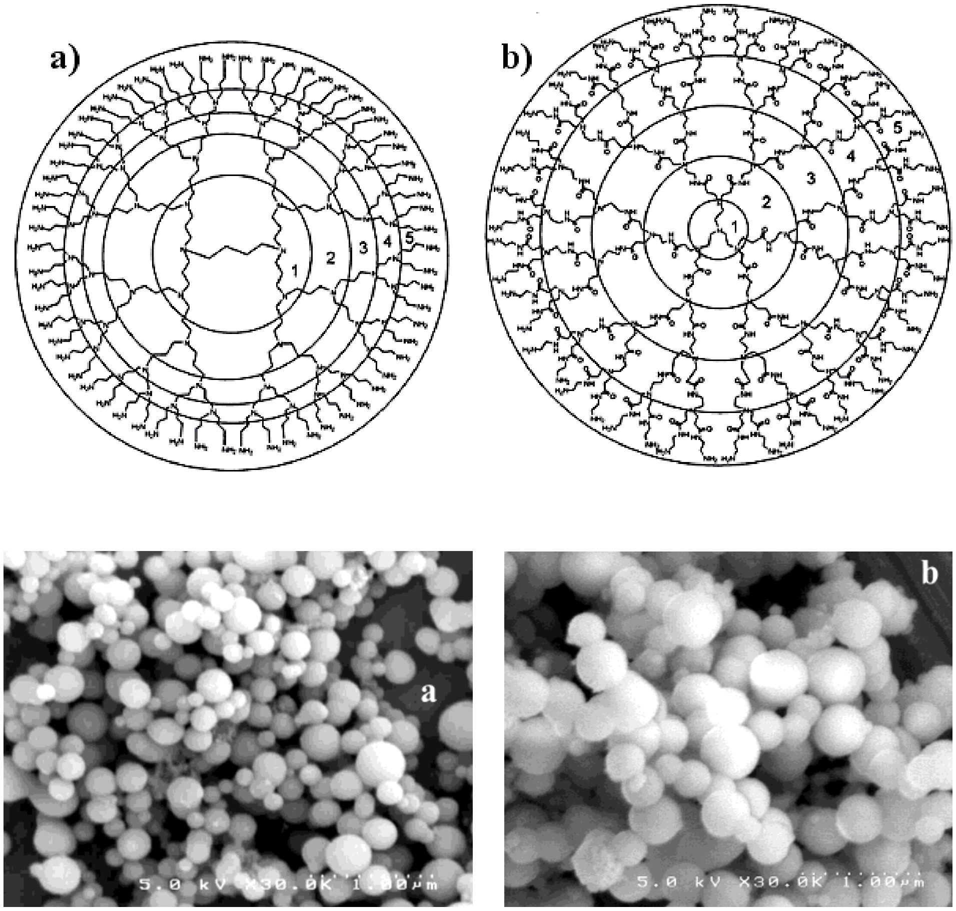

Figure 1. 11. Chemical structures of G-5 PPI dendrimer (a) and G-5 PAMAM dendrimer (b) and SEM micrographs of silica nanoparticles formed by (a) G4 PPI and (b) G4 PAMAM dendrimers [85].

To obtain covalently cross-linked, three-dimensional nanodomained dendrimer-based networks, Dvornic *et al* [83, 102] functionalized hydrophilic PAMAM dendrimers with hydrophobic organosilicons (OS), such as alkoxysilanes, to form a new family of radially layered copolymeric PAMAMOS dendrimers. The hydrolysis and polycondensation of these PAMAMOS dendrimers formed three-dimensional, covalently bonded, nanostructured networks containing well-defined shapes and sizes of intermeshed hydrophilic and hydrophobic nanosopic domains of PAMAM dendrimers and OS domains (Figure 1.12). The properties of these networks depend on different parameters including compositions and structures of different type of organosilicon reagent, the generation number of PAMAM dendrimers, and processing procedures.

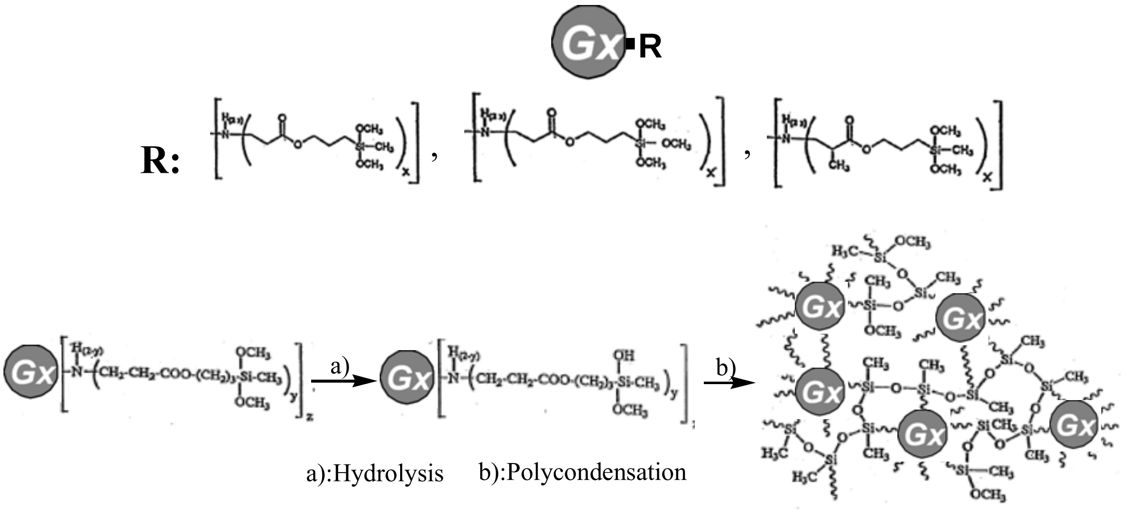

Figure 1. 12. Alkoxysilyl functionalized PAMAM dendrimers and the mechanism of hydrolysis and condensation reactions [102].

The conventional removal of dendrimer templates by calcination, a process leading to decomposition of dendrimer structures at high temperature, leaves cavities in amorphous silica networks to produce nanoporous materials [81, 82, 84]. For example, Larsen *et al* [81] used the G-4 PAMAM amine dendrimers as templates to synthesize amorphous silica gels from tetraethyl orthosilicate (TEOS) *via* the sol-gel method. The removal of dendrimers by calcination produced cavities in silica networks, which were characterized by X-ray diffraction and nitrogen adsorption method. Pakkanen *et al* [100] prepared amorphous silica material through neutral templating route by using amine-terminated templates based on hydrogen-bonding interactions between neutral amines and neutral inorganic precursors. TEOS was added slowly into the solution of three kinds of template dendrimer core molecules: tris(2-aminoethyl)amine (1), low molecular weight polyamidoamine-type dendrimer (2), and low molecular weight dendrimer derived from pentaerythritol (3) (Figure 1.13) to prepare silica materials. The templates were removed by calcination at different temperatures. These silica networks were characterized by nitrogen absorption, X-ray diffraction, and TGA measurement. Figure 1.14 shows the synthetic procedure for silica networks using dendrimers as templates.

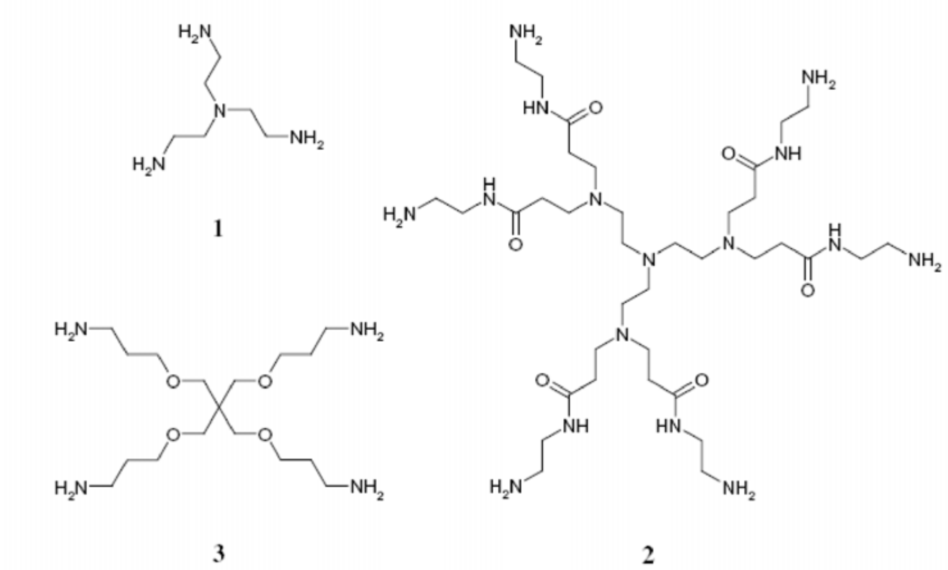

Figure 1. 13. Representatives of dendrimer core molecules [100].

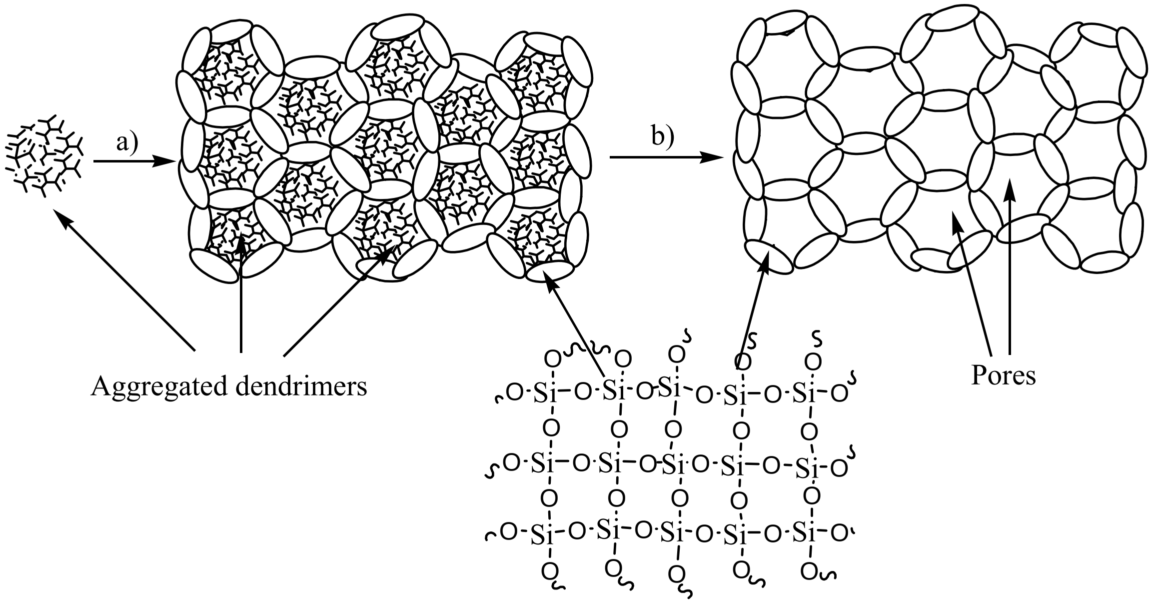

Figure 1. 14. Representative of the synthetic procedure of silica networks using dendrimers as templates: a) construction of silica networks around aggregated dendrimers; b) removal of dendrimer templates.

1.3 Characterization

Silica hybrid networks are characterized using a combination of techniques including solid-state ^{29}Si & ^{13}C NMR and FT-IR spectroscopes, as well as nitrogen absorption-desorption, TEM, and X-ray diffraction, etc [103]. These techniques provide information related to silica network morphological features. A brief introduction to these measurement techniques is provided below.

1.3.1 Solid-State ^{29}Si & ^{13}C {^{1}H} Nuclear Magnetic Resonance (NMR)

Silica materials have been intensively studied using solid-state ^{29}Si NMR [104, 105]. The type of Si-O-Si links in sol-gel materials can be easily determined by this technique. A tetrahedrally bonded silica network will be formed if four silicon alkoxide react completely after hydrolysis, otherwise, either incomplete hydrolysis or polycondensation resulting in not-fully-formed-silica network. The latter can be observed in the isotropic chemical shifts of high-resolution solid-state ^{29}Si spectra. The various type of silicate structures have been characterized using the symbols of "Q" ($Q=Si(O_{1/2})_4$), "T"($T= Si(O_{1/2})_3R$), and "D" ($D= Si(O_{1/2})_2R_2$) [106]. For silica networks containing oxygen and organic groups "R", "Q" represents quaternary oxygen, "T" represents three oxygens and one organic group "R", "D" represents two oxygens and two organic groups "R" (Figure 1.15). The corresponding isotropic chemical shifts range for ^{29}Si NMR resonances of various silicate structures were compiled by Glaser et al [106], and a list is presented in (Table 1.1).

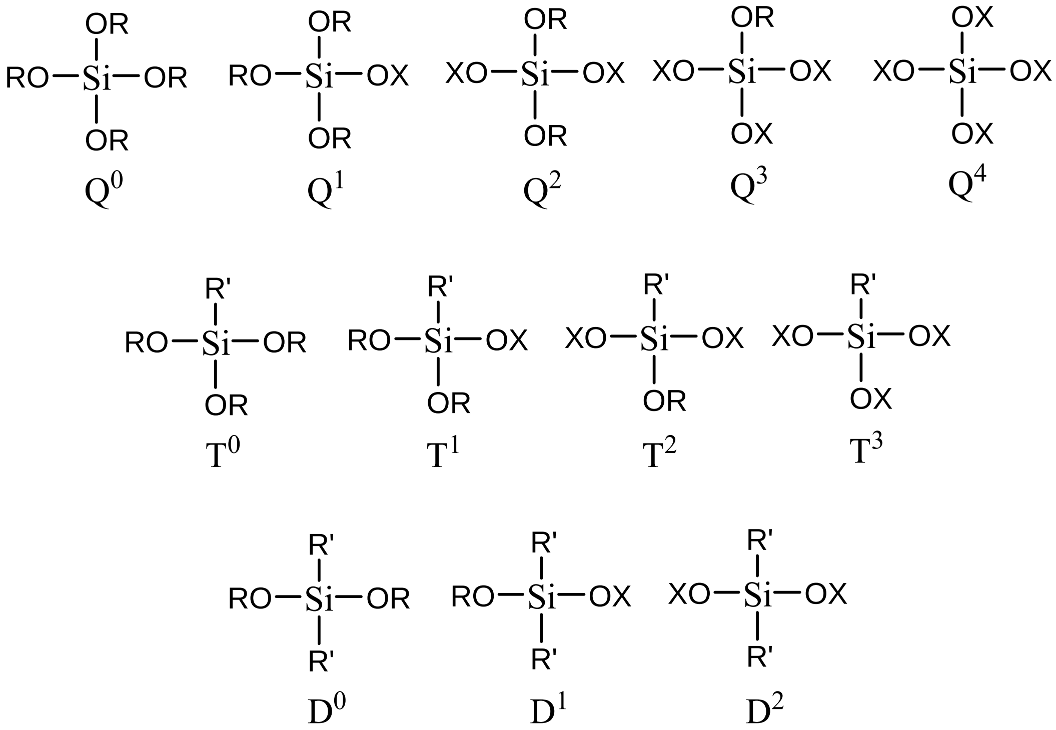

Figure 1. 15. Possible silicate structures in the silica-based networks: R, alkyl group or H; X, quaternary Si. Modified from reference [106].

Table 1. 1. ^{29}Si chemical shift (-δ, ppm) for silicate structures synthesized from the sol-gel process [106].

Q^4	Q^3	Q^2	Q^1	Q^0	T^3	T^2	D^2	D^1
107-110	90-100	83-88	78-83	66-74	65-66	55-56	19	12
109.3	99.8	90.6		75-85	55-66	56	19-23	8-9
99-10	99	89			62-64	53-57	16-18	
106-110	98-101	89			61-64	55-56	13-18	
105-108	98-100							

Solid-state ^{13}C {^1H} NMR spectroscopy is also a valuable technique to study the organic moieties in silica networks. The chemical shifts, which depend on the specific organic molecules, can be used to confirm their presence and the types of carbon structures present in silica-based networks [105].

1.3.2. FT-IR Spectroscopy (FT-IR)

Fourier Transform Infrared Spectroscopy (FT-IR) is a powerful tool to identify different types of chemical bonds in an organic or inorganic molecule. Infrared radiation in the range of 666-4000 cm^{-1} is absorbed by organic or inorganic molecules, and is converted into energy of molecular vibrations. These vibrations, that are of two types, *stretching* and *bending*, induce a rhythmical change in the dipole moment of the molecule to be observed [107]. For silica-based networks, FT-IR spectra should contain the band corresponding to Si-O-Si stretching (broad strong peak at around 1088 cm^{-1}) and Si-OH (medium peak at around 3400 cm^{-1}). The peaks corresponding to Si-C (stretching at around 800 cm^{-1}, asymmetric at around 1410 cm^{-1}, and symmetric at around 1260 cm^{-1}) should be observed if the organic residues are still present in silica-based networks.

1.3.3 Transmission Electron Microscopy (TEM)

TEM is a powerful tool to obtain essential information about typical mesoparticle size and shape, porosity and morphological features of silica-based networks [103]. The image that can be seen on the screen is the result of differential loss of electrons from a beam transmitted through a thin-film sample. A stream of monochromatic electrons from a source (electron gun) is focused on to a small, thin, coherent beam by electromagnetic condenser lens. The beam, which strikes and passes through the sample, is focused by the objective lens into an image on a fluorescent screen, or an image converter plate. In TEM, the electrons that travel through the specimen are channeled and focused through a series of different lenses, among which the objective lens and the intermediate lens are the most important. Variations in the current passing through the objective lens can produce changes in the focal length, which brings the final magnified image into focus [108].

1.3.4. Surface Area Measurement

Methods such as Langmuir [109] and BET [110] methods are used to calculate the surface area of solid materials. These are based on the isothermal adsorption of gas, such as nitrogen. The BET method, which was introduced by Brunauer, Emmett, and Teller (BET), has been established for many years. It is an extension of the Langmuir theory, which relates to monolayer molecular adsorption to multilayer adsorption. This multilayer adsorption method could be used to measure the total surface area of silica materials.

The linear BET equation is given by:

$$\frac{P}{V(P_0 - P)} = \frac{1}{V_m C} + \frac{C-1}{V_m C} \times \frac{P}{P_0} \qquad (1)$$

Where: V_m = Volume of the monolayer
V = Volume adsorbed
P = Sample pressure
P_0 = Saturation vapor pressure

The BET surface area is then calculated using the following equation:

$$SA = V_m \times N \times A_m \qquad (2)$$

Where: SA = Surface area of the sample
V_m = Volume of adsorbed monolayer
N = Avogadro's number
A_m = Cross-sectional area of the adsorbate molecule

If nitrogen is used, the default value of A_m is 16.2 A_2 and the equation (2) is simplified to:

$$SA = 4.35 \times V_m \left(\frac{M^2}{g} \right) \qquad (3)$$

1.3.5 X-ray Powder Diffraction (XRPD)

X-ray diffraction is one of the most important characterization tools used in solid-state chemistry and materials science. X-rays, which are electromagnetic radiation of wavelength about 1 Å, are used to probe crystalline structures at the atomic level. They primarily interact with electrons in atoms. Some photons from the incident beam will be deflected away from the direction where they originally travel. Diffracted waves from different atoms can interfere with each other and the resultant intensity distribution is strongly modulated by this interaction. If the atoms are arranged in a periodic fashion, as in crystals, the diffracted waves will consist of sharp interference peaks with the same symmetry as in the distribution of atoms (Figure 1.16). These peaks in an X-ray diffraction pattern are directly related to the atomic distances (*d*), which can be determined by Bragg's equation:

$$n\lambda = 2d\sin\theta \qquad (4)$$

Where: λ = the wavelength of the X-ray

θ = the scattering angle

n = an integer representing the order of the diffraction peak

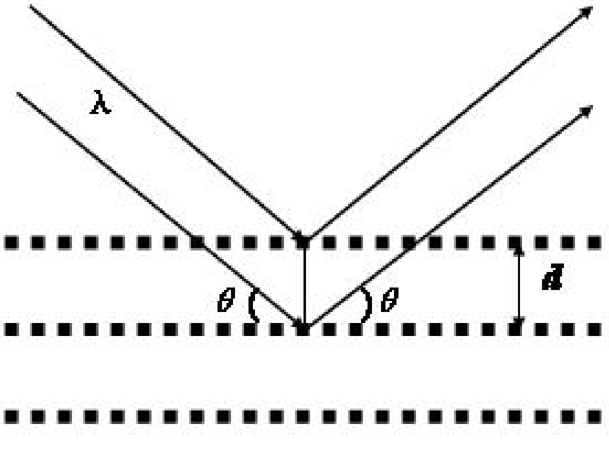

Figure 1. 16. Reflection of X-rays from two planes of atoms in a solid.

X-ray diffraction has been in use in two main areas, for characterization of crystalline materials and the determination of their structure. Each crystalline solid has its unique characteristic X-ray powder pattern, which may be used as a "fingerprint" for its identification. Once the material has been identified, X-ray crystallography may be used to determine its structure. The Powder XRD (XRPD) is the most widely used X-ray diffraction technique for characterizing materials. The term “powder” means that the crystalline domains are randomly oriented in the sample. Therefore when the 2D diffraction pattern is recorded, it shows concentric rings of scattering peaks corresponding to the various d spaces in the crystal lattice. The positions and the intensities of the peaks are used for identifying the underlying structure (or phase) of the materials [111].

References

1. J. Pinkas, *Ceramics-Silikaty*, 2005. **4**: p. 287.
2. T. Uchino, *J. of the Ceramic Society of Japan*, 2005. **1**: p. 17.
3. G. J. de A. A. Soler-Illia, C. Sanchez, B. Lebeau and J. Patarin, *Chem.Rev.*, 2002. **102**: p. 4093.
4. G. A. Ozin, *Adv. Mater.*, 1992. **4**: p. 612.
5. B. Hatton, K. Landskron, W. Whitnall, D. Perovic and G. A. Ozin, *Acc. Chem. Res.*, 2005. **38**: p. 305.
6. C. T. Kresge, M. E. Leonowicz, W. J. Roth, J. C. Vartuli and J.S. Beck, *Nature*, 1992. **359**: p. 710.
7. J. S. Beck, J. C. Vartuli, G. J. Kennedy, C. T. Kresge, W. J. Roth and S. F. Schramm, *Chem. Mater.*, 1994. **6**: p. 1816.
8. L. L. Hench and J. K. West, *Chem. Rev*, 1990. **90**: p. 33.
9. J. T. Davis and E. K. Rideal, *In Interfacial Phenomena, Academic Press: New York*, 1963.
10. C. J. Brinker and G. W. Scherer, *Sol-Gel Science, Academic Press, San Diego.* 1990.
11. W. Alain, *Electroanalysis*, 2001. **13**(8-9): p. 701
12. T. Graham, *J. Chem. Soc.* 1864. **17**: p. 318
13. B. E. Yoldas, *Bull. Am. Ceram. Soc.*, 1975. **54**: p. 286.
14. P. J. Flory, *Priciples of Polymer Chemistry, Cornell University Press; Ithaca,NY; Chapter IX.* 1953.
15. J. Livage, *Currant opinion solid state & materials science*, 1997. **2**: p. 132.
16. M. Ebelmen, *Ann. Chimie Phys.*, 1846. **16**: p. 129.
17. M. Ebelmen, *C. R. Acad. Sci.*, 1847. **25**: p. 854.
18. A. Walcarius, *Electroanalysis*, 2001. **13**: p. 701.
19. C. Sanchez, G. J. de A. A. Soler-Illia, F. Ribot, T. Lalot, C. R. Mayer and V. Cabuil, *Chem. Mater.*, 2001. **13**: p. 3061.
20. J. Wen and G. L. Wilkes, *Chem. Mater.*, 1996. **8**: p. 1667.
21. H. Schmidt, *J. Non-Cryst. Solids*, 1984. **63**: p. 1.

22. H. Schmidt, *J. Non-Cryst. Solids*, 1984. **63**: p. 283.
23. H. Schmidt, *Mater. Res. Soc. Symp. Proc.*, 1984. **32**: p. 327.
24. H. Schmidt, *J. Non-Cryst. Solids*, 1985. **73**: p. 681.
25. G. L. Wilkes, B. Orler and H. Huang, *Polym. Prepr.*, 1985. **26**: p. 300.
26. G. L. Wilkes, A. B. Brenann, H. Huang, D. Rodrigues and B. Wang, *Mater. Res. Soc. Symp. Proc.*, 1990. **171**: p. 15.
27. G. L. Wilkes, H. Huang and R. H. Glaser, *Silicon-Based Polymer Science: A Comprehensive Resource*; Advances in Chemistry Ser. 224; American Chemical Society: Washington DC, 1990: p. 207.
28. J. E. Mark, *Chemtech.*, 1989. **19**: p. 230.
29. J. E. Mark, S. Wang, P. Xu and J. Wen, *J. Mater. Res. Soc. Symp. Proc.*, 1992. **274**: p. 77.
30. J. E. Mark and P. D. Calvert, *J. Mater. Sci., Part C*, 1994. **1**: p. 159.
31. D. Avnir, D. Levy and R. Reisfeld, *J. Phys. Chem.*, 1984. **88**: p. 5956.
32. D. Levy, S. Einhorn and D. Avnir, *J. Non-Cryst. Solids*, 1989. **113**: p. 137.
33. F. Hof, S. L. Craig, C. Nuckolls and J. Rubek, *Angew. Chem. Int. Ed. Engl.*, 2002. **41**: p. 1488.
34. C.-Y. Su, M. D. Simth and H.-C. Loyle, *Angew. Chem., Int. Ed. Engl.*, 2003. **42**: p. 4085.
35. P. J. Branton, P. G. Hull and K. S. W. King, *J. Chem. Soc., Chem. Commun.*, 1993: p. 1257.
36. K. Moller and T. Bein, *Chem. Mater.*, 1998. **10**: p.2950.
37. J. Y. Kim, S. B. Yoon and J. S. Yu, *Chem. Mater.*, 2003. **15**: p. 1932.
38. G. A. Ozin, *Chem. Commun.*, 2000. p. 419
39. C. -Y. Lai, B. G. Treyn, D. M. Jeftinija, K. Jeftinija, S. Xu and V.S.-Y. Lin, *J. Am. Chem.*, 2003. **125**: p. 4451.
40. L. R. Nassimbeni, *Acc. Chem. Res.*, 2003. **36**: p. 631.
41. S. Mann, S. L. Burkett, S. A. Davis, C. E. Fowler, N. H. Mendelson, S. D. Sims, D. Walsh and N. T. Whilton, *Chem. Mater.*, 1997. **9**: p. 2300.
42. J. S. Beck and J.C. Vartuli, *Curr. Opinion in Solid State and Materials Science*, 1996. **1**: p. 76.

43. B. Boury, P. Chevalier, R. J. P. Corriu, P. Delord, J. J. E. Moreau and M. W. Chiman, *Chem. Mater.*, 1999. **11**: p. 281.

44. A. Berggren, A. E. C. Palmqvist and K. Holmberg, *Soft Matter*, 2005. **1**: p. 219.

45. N. K. Raman, M.T. Anderson and C. J. Brinker, *Chem. Mater.*, 1996. **8**: p. 1682.

46. Q. Huo, D. I. Margolese, U. Ciesla, D. G. Demuth, P. Feng, T. E. Gier, P. Sieger, A. Firouzi, B. F. Chmelka, F. SchEth and G. D. Stucky, *Chem. Mater.*, 1994. **6**: p. 1176.

47. P. T. Tanev, T.J.Pinnavaia, *Science*, 1995. **267**: p. 865.

48. J. S. Beck, J. C. Vartuli, W. J. Roth, M. E. Leonowicz, C. T. Kresge, K. D. Schmitt, C. T. W. Chu, D. H. Olson, E. W. Sheppard, et al., *J. Am. Chem.Soc.*, 1992. **114**: p. 10834.

49. T. S. Yanagisawa, K. Kuroda and C. Kato, *Bull. Chem. Soc. Jpn*, 1990. **63**: p. 988.

50. S. Inagaki, Y. Fukushima and K. Kuroda, *J. Chem. Soc., Chem. Commun.*, 1993: p. 680.

51. F. Hoffmann, M. Cornelius, J. Morell and M. Froba, *Angew. Chem. Int. Ed.*, 2006. **45**: p. 3216.

52. Y. M. Setoguchi, Y. Teraoka, I. Moriguchi, S. Kagawa, N. Tomonaga, A. Yasutake and J. Izumi, *J. Porous Mater.*, 1997. **4**: p. 129.

53. S. Shio, A. Kimura, M. Yamaguchi, K. Yoshida and K. Kuroda, *Chem. Commun.*, 1998: p. 2461.

54. G. S. Attard, J. C. Glyde and C. G. GVltner, *Nature*, 1995. **378**: p. 366.

55. A. Monnier, F. SchEth, Q. Huo, D. Kumar, D. Margolese, R. S. Maxwell, G. Stucky, M. Krishnamurty, P. Petroff, A. Firouzi, M. Janicke and B. Chmelka, *Science*, 1993. **261**: p. 1299.

56. Q. Huo, D. I. Margolese, U. Ciesla, P. Feng, T. E. Gier, P. Sieger, R. Leon, P. M. Petroff, F. SchEth and G. D. Stucky, *Nature*, 1994. **368**: p. 317.

57. Q. Huo, R. Leon, P. M. Petroff and G. D. Stucky, *Science*, 1995. **268**: p. 317.

58. S. A. Bagshaw, E. Prouzet and T. J. Pinnavaia, *Science*, 1995. **269**: p. 1242.

59. D. Zhao, J. Feng, Q. Huo, N. Melosh, G. H. Frederickson, B. F. Chmelka and G. D. Stucky, 1998. **279**: p. 548.

60. R. Ryoo and C. H. Ko, *J. Phys. Chem. B*, 2000. **104**: p. 11465.

61. S. Förster and M. Antonietti, *Adv.Mater.*, 1998. **10**: p. 195.
62. D. Y. Zhao, Q. S. Huo, J. L. Feng, B. F. Chmelka and G. D. Stucky, *J. Am. Chem. Soc.*, 1998. **120**: p. 6024.
63. Z. W. Jin, X. D. Wang and X. G. Cui, *J. Mater. Sci.*, 2007. **42**: p. 465.
64. S.-Y. Chen and S. Cen, *Chem. Mater.*, 2007. **19**: p. 3041.
65. F. Kleitz, D. N. Liu, G. M. Anilkumar, In-Soo Park, L. A. Solovyov, A. N. Shmakov and R. Ryoo, *J. Phys. Chem.* B, 2003. **107**: p. 14296.
66. M. J. Adeogun, J. P. A. Fairclough, J. N. Hay and A. J. Ryan, *J. of Sol-Gel Sci. and Technol.*, 1998. **13**: p. 27.
67. M. J. Adeogun and J. N. Ryan, *Polym. Int.*, 1996. **41**: p. 123.
68. M. J. Adeogun and J. N. Ryan., *Chem. Mater.*, 2000. **12**: p. 767.
69. M. Fisher and F. Vogtle, *Angew. Chem. Int. Ed. Engl.* , 1999. **38**: p. 884.
70. A. K. Patri, I. J. Majoros and J. R. Baker, *Current Opinion in Chmeicla Biology*, 2002. **6**: p. 466.
71. G. R. Newkome, E. He and C. N. Moorefield, *Chem. Rev.*, 1999. **99**: p. 1689.
72. F. Vögtle, *Topics in Current Chemistry*, 1998. **197**: p. 7.
73. J. H. G. Jansen, E. W. Meijer and E. M. Brabander-van der Berg, *J. Am. Chem. Soc.*, 1995. **117**: p. 4417.
74. S. C. Zimmerman, Y. Wang and J. Moore, *J. Chem. Soc., Chem. Commun.* , 1998. **120**: p. 2172.
75. R. van Heerbeek, P. C. J. Kamer, P. W. N. M. van Leeuwen and J. N. H. Reek, *Chem. Rev.*, 2002. **102**: p. 3717.
76. J. W. J. Knapen, A. W. van der Made, J. C. de Wilde, P. W. N. M. van Leeuwen, P. Wijkens, D. M. Grove and G. van Koten, *Nature*, 1994. **372**: p. 659.
77. E. I. KO, *CHEMTECH*, 1993. **23**: p. 31.
78. E. Linder, M. Kemmler, H. A. Mayer and P. J. Wegner, *J. Am. Chem. Soc.* , 1994. **116**: p. 348.
79. U. Schubert, N. Husing and A. Lorenz, *Chem. Mater.*, 1995. **7**: p. 2010.
80. A. A. Czerniewski, X. J. Liu, O. Rolland, R. Hourani, M. Four and A. Kakkar, *J. Mater. Chem.*. **17**(26): p. 2737-2745.
81. G. Larsen, E. Lotero and M. Marquez, *J. Phys. Chem. B*, 2000. **104**: p. 4840.

82. S. Jahromi and B. Mostert, *Macromolecules*, 2004. **37**: p. 2159.

83. P. R. Dvornic, R. A. Bubeck, S. D. Reeves, J. Li and L. W. Hoffman, *Silicon Chemistry*, 2003. **2**: p. 207.

84. A. M. Caminade and J. P. Majoral, *Acc. Chem. Res.,* 2004. **37**(6): p. 341.

85. M. R. Knecht and D. W. Wright, *Langmuir*, 2004. **20**: p. 4728.

86. M. R. Knecht, S. L. Sewell and D. W. Wright, *Langmuir*, 2005. **21**: p. 2058.

87. A. M. Caminade and J. P. Majoral, *J. Mater. Chem.* 2005. **15**: p. 3643.

88. Y. Chujo, H. Matsuki, S. Kure, T. Saegusa and T. Yazawa, *J. Chem. Soc., Chem. Commun.*, 1994. **5**: p. 635.

89. B. Boury, R. J. P. Corriu and R. Nunez, *Chem. Mater.,* 1998. **10** (7): p. 1795.

90. J. W. Kriesel and T. D. Tilley, *Chem. Mater.,* 1999. **11**(5): p. 1190.

91. J. W. Kriesel and T. D. Tilley, *Chem. Mater.*, 2000. **12** (4): p. 1171.

92. K. G. Sharp and M. J. Michalczyk, *J. Sol-Gel Science and Technology*, 1997. **8**(1): p. 541.

93. D. Y. Son, *The Chemistry of Organic Silicon Compounds, Chapter 13. Edited by Zvi Rappoport and Yitzhak Apeloig, John Wiley & Sons, Ltd.* 2001. **3**: p. 745.

94. K. J. Shea, D. A. Loy and O. Webster, *J. Am. Chem. Soc.*, 1992. **114**: p. 6700.

95. B. K Cho, A. Jain, S. M. Gruner and U. Wiesner, *Chem. Mater.,* 2007. **19** (15): p. 3611.

96. S. Volden, W. R. Glomm, H. Magnusson, G. Qye and J. Sjoblom, *J. of Dispersion Science and Technology*, 2006. **27**: p. 893.

97. S. A. Miller, E. D. Hong and D. Wright, *Macromolecular Bioscience*, 2006. **6** (10): p. 839.

98. B. Zhang and J.Wang, *Nanoscience*, 2006. **11**: p. 114.

99. A. Bouchara, L. Rozes, G. J. de A.A. Soler-Illia, C. Sanchez, C. O. Turrin, A. M. Caminade and J. P. Majoral, *Journal of Sol-Gel Science and Technology,* 2003. **26**(1): p. 629.

100. J. Hukkamaki and T. T. Pakkanen, *Microporous and Mesoporous Materials*, 2003. **65**(2-3): p. 189.

101. Eli Ruckenstein and W.Yin, *J. Poly. Sci. Part A: Poly.r Chem.,* 2000. **38** (9): p. 1443.

102. P. R. Dvornic, J. Li, A. M. de Leuze-Jallouli, S. D. Reeves and M. J. Owen, *Macromolecules*, 2002. **35** (25): p. 9323.

103. R. M. Stroud, J. W. Long, J. J. Pietron and D. R. Rolison, *Journal of Non-Crystalline Solids,* 2004. **350**: p. 277.

104. R. Simonutti, A. Comotti, F. Negroni and P. Sozzani, *Chem. Mater.* 1999. **11** (3): p. 822.

105. R. Simonutti, A. Comotti, S. Bracco and P. Sozzani, *Chem. Mater.* 2001. **13** (3): p. 771.

106. R. H. Glaser, G. L. Wilkes and C. E. Bronnimann, *Journal of Non-Crystalline Solids*, 1989. **113**(1): p. 73.

107. N. B. Colthup, L. H. Daly, S. E. Wiberley, *Introduction to infrared and Raman spectroscopy. Boston: Academic Press.* 1990.

108. G. Thomas, M.J.Goringe, *Transmission electron microscopy of materials. New York: John Wiley & Sons.* 1979.

109. I. Langmuir, *J. Am. Chem. Soc.*, 1918. **40**: p. 1368.

110. S. Brunauer, P. H. Emmett and E. Teller, *J. Am. Chem. Soc.*, 1938. **60**: p. 309-319.

111. R. Jenkins and R. L. Snyder, *Introduction to X-ray powder diffractometer, New York: Wiley.* 1996.

Chapter 2: Templating Silica Network Construction Using 3,5-Dihydroxybenzyl alcohol Based Dendrimers: Influence of Dendrimer Aggregation on Evolving Network Structure

(*Journal of Materials Chemistry*, 2007, **17**, 2737-2745)

Contribution of Authors

Alex Adam Czerniewski, Olivier Rolland and Mickael Four were undergraduate students in the group, and each had done a limited study of networks as a part of their undergraduate research. I made the major contribution to this study by carrying out a detailed synthesis of dendrimers and their corresponding dendrimer templated silica networks, using two different types of silane reagents, characterization using a variety of complimentary techniques, and then examined their potential in small molecule encapsulation.

2.1 Introduction

Highly cross-linked network materials with a desired porous internal environment continue to arouse intense scientific interest for a variety of applications including molecular encapsulation, selective catalysis, drug delivery etc [1-2]. Such systems that can provide complementarity in terms of size and shape between the network host and incoming guest will lead to pathways for predicting and controlling their release profile [1,3,4]. Numerous methods to achieve this goal have been used in the past that have employed surfactants, polymers, colloidal particles etc as templates for creating pores with controlled structural features [5,6]. Dendritic macromolecules that are monodisperse in nature possess properties that are ideally suited for constructing such networks. Dendrimers are composed of a multivalent core where branched, wedge-like structures called dendrons emerge radially towards the periphery, and their size, shape and terminal units of the branches can be efficiently controlled [7-9]. The resulting flexibility in tailoring dendrimer architecture provides advantages in using them as core units to prepare desired materials. Several attempts to create such networks using dendrimers as templates have recently been reported, and have provided great impetus in constructing *smart* hybrid materials using dendritic macromolecules [10-18]. The synthesis of these networks is carried out by hydrolysis and condensation of the dendrimer-periphery grafted silicon-alkoxy groups, and the subsequent removal of the templates by calcification. The morphology of the resulting networks is thought to be directed by the individual spherical dendrimers, and much of the emphasis in this regard has been placed in controlling the internal structure by employing the appropriate dendrimer generation. An important factor that is generally overlooked is the role of dendritic intermolecular interactions prior to network synthesis, on the build-up of network structure and the surface morphology of the resulting hybrid materials. The strength of such interactions, as expected, is dictated by the nature of the peripheral dendritic groups. Dendrimers with peripheral groups that can participate in hydrogen bonding will be more prone to aggregation in solution, and thus strongly influence the formation of hybrid materials. Since, in general, synthesis of the networks is carried out at concentrations well above those required for the inter-dendrimer interactions, we were intrigued by the influence of the supramolecular chemistry of dendrimers prior to silica network construction, on the overall structure of the resulting networks. We report herein a simple methodology to prepare silica based networks using 3,5-dihydroxybenzylalcohol (DHBA) based dendrimers as templates, and demonstrate the role of dendrimer aggregation and the type of silane reagent employed in the reaction, on the evolution of the network structure. DHBA and its corresponding dendrimers contain peripheral hydroxyl groups that increase exponentially upon an increase in generation number, and are known to promote aggregation *via* intermolecular hydrogen bonds [19-21]. Dendrimer generation and its ability to aggregate can thus significantly influence the morphology of the resultant networks. In addition, the choice of the silane reagent ($Si(NMe_2)_4$ or $ClSi(NEt_2)_3$) employed for the process also plays an important role in the evolution of the network. The reaction sequence of the silane reagent in a mild sol-gel methodology [22-23], leads to highly cross-linked networks from which dendrimer templates are removed upon further treatment with HCl or *in situ*. The residual Si-OH groups, upon removal of the templates, are directed inwards, making these networks, intriguingly, water repellent on their surface with a hydrophilic interior. These features may provide flexibility in adapting to the specific encapsulation needs of different target molecules [8,24-31].

2.2 Results and Discussion

DHBA based dendrimers of generations 1-5 (Figure 2.1) were prepared from commercially available DHBA using a divergent synthetic methodology, and details of the synthesis and characterization of these dendrimers have been reported earlier [19-21,32-33]. The dendritic growth is carried out by a repetitive and controlled coupling reaction of $Me_2Si(NMe_2)_2$ with DHBA's terminal OH groups, leading to the formation of Si-O links, with gaseous methylamine as the only by-product. The size of these dendrimers is dependent on their generation number with diameters ranging from 16Å to 75Å, and in general, these dendrimers assume a more globular shape as the generation number increases [21]. Dendrimers of generations 1-3 form aggregates above a critical aggregation concentration (*cac*) of 3.7 mg/mL while generation 4 and 5 dendrimers aggregate even at much lower concentrations [19-21].

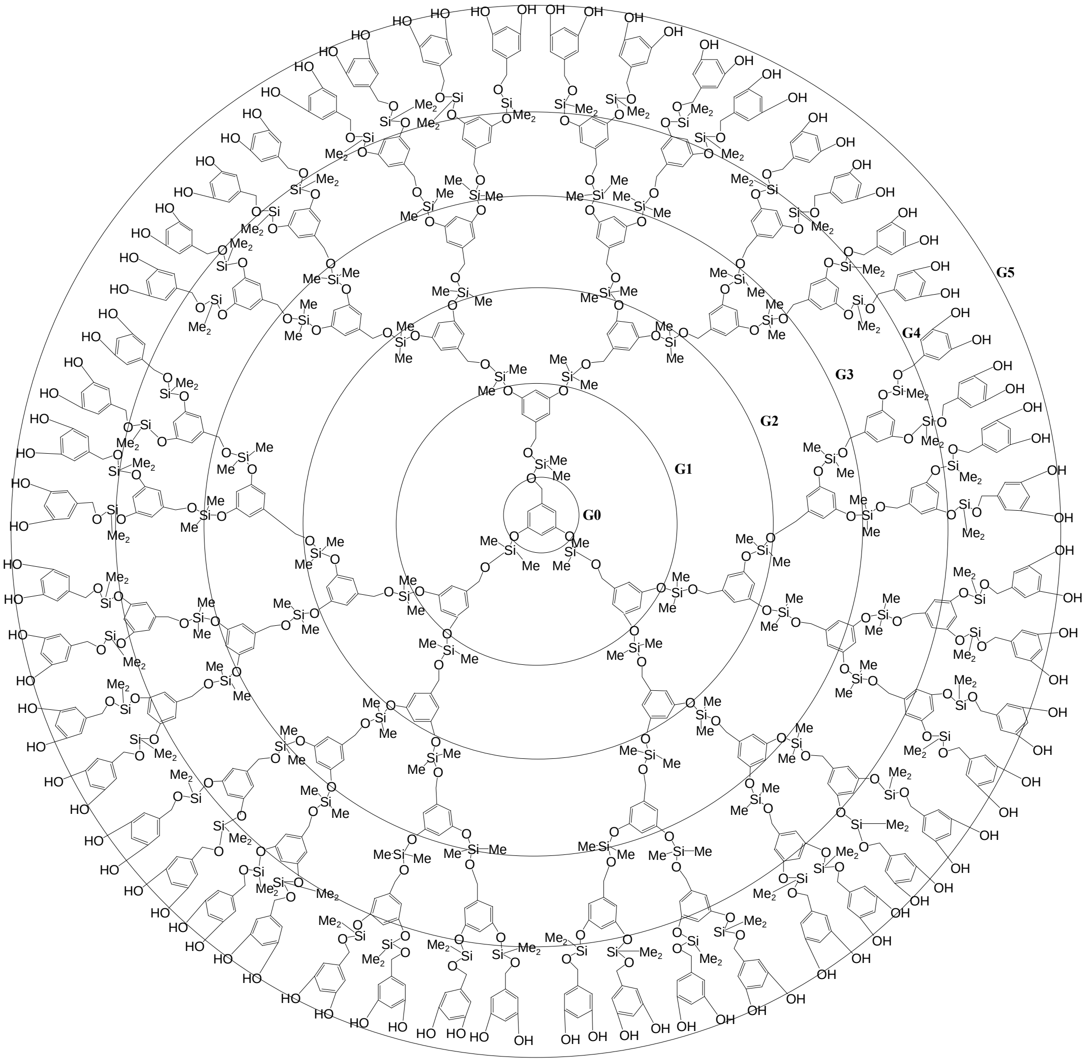

Figure 2. 1. Schematic representation of generations of 0-5 (G0-G5) 3,5-dihydroxybenzyl alcohol (DHBA) based dendrimers.

The synthesis of dendrimer-templated networks was achieved using a sol-gel poly-condensation process that utilizes milder aminosilane reagents (Scheme 2.1) compared with chloro-silanes ($SiCl_4$) that are commonly used in the construction of silica [22-23]. It involves, in the first step, simple acid-base hydrolytic chemistry of aminosilanes with the terminal hydroxyl groups of the dendrimers. This is followed by the hydrolysis of the remaining $Si\text{-}NR_2$ groups into Si-OH groups, subsequent condensation of which results in a Si-O-Si network formation. The condensation process is facilitated by the base, HNR_2, formed as a by-product, in the first step. Aminosilane reagents that were employed in this study included tetrakis(dimethylamino)silane ($Si(NMe_2)_4$) and chlorotris(diethylamino)silane ($ClSi(NEt_2)_3$). $Si(NMe_2)_4$ is commercially available, and $ClSi(NEt_2)_3$ was prepared *in situ* from tetrachlorosilane and diethylamine. The extent of silica network formation was controlled by the amount of aminosilane reagent used in the reaction.

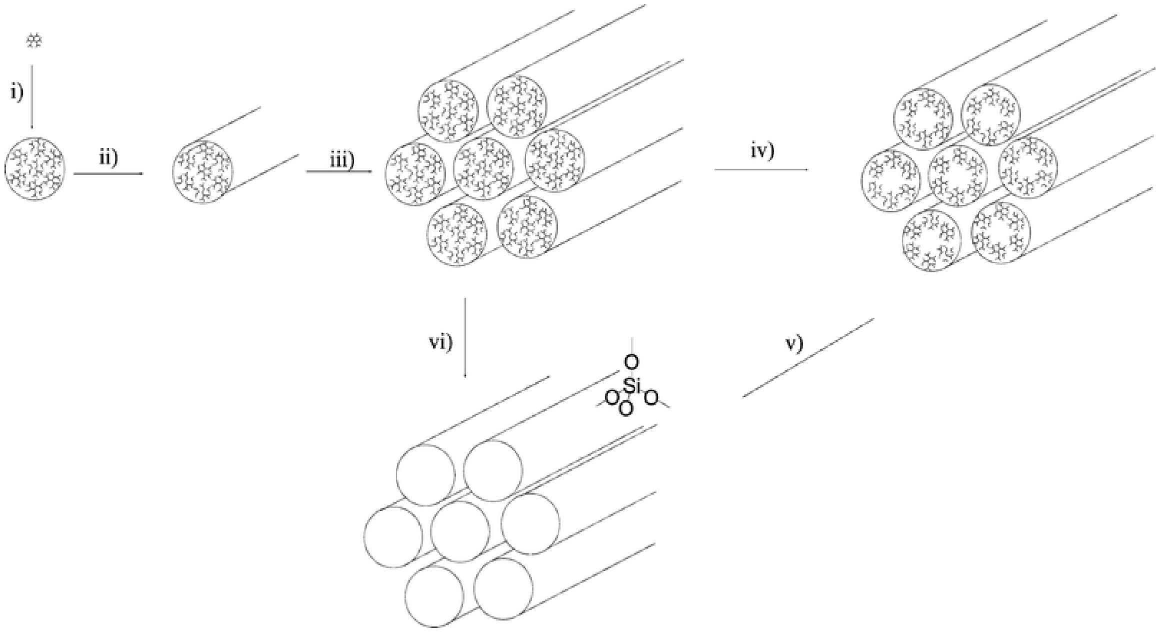

Scheme 2. 1. Construction of dendrimer templated networks: (i) aggregation of dendrimers in solution; (ii) formation of silica networks around aggregated dendrimers; (iii) condensation of silica networks; (iv) leaching of internal aggregated dendrimers; (v) removal of dendrimer templates by HCl treatment; (vi) *in situ* removal of dendrimer templates.

In general, for every hydroxyl group present in the template, 1 equivalent of aminosilane reagent was employed. For example, generation 1 dendrimer (G1) has six hydroxyl groups available and hence 6 equivalents of the silane reagent were used for the reaction. The concentrations of dendrimer solutions were those at which they form aggregates since highly dilute solutions at which these dendrimers exist as individual molecules, are not prone to polycondensation for network formation. The preparation of dendrimers-templated networks using $Si(NMe_2)_4$ was slow, whereas, the high reactivity of $ClSi(NEt_2)_3$ enables network formation in 48-72 h. As expected, these networks were generally insoluble in common laboratory solvents.

2.2.1 Dendrimer Templated Networks Prepared Using $Si(NMe_2)_4$

Solid-State $^{13}C\{^1H\}$ NMR spectroscopy is a useful technique to confirm the presence of dendrimer templates in the networks [27]. For example, for DHBA-based networks prepared with $Si(NMe_2)_4$, the solid state $^{13}C\{^1H\}$-NMR spectra typically showed peaks around 25 ppm (for $SiMe_2$), 65 ppm for C_6H_3-$\mathit{C}H_2OSi$, and five peaks in the region between 100 and 158 ppm for C_6H_3 corresponding to the DHBA backbone. It is known that alkoxysilane bonds (Si-OR) can be hydrolyzed under acidic conditions. Thus, the dendrimer moieties in the networks prepared using $Si(NMe_2)_4$ were removed by placing them in dilute (1%) HCl solutions. The removal of the dendritic fractions in these types of networks was confirmed by the complete disappearance of the above mentioned peaks in their solid-state $^{13}C\{^1H\}$spectra.

Solid-state ^{29}Si-NMR spectroscopy is an extremely valuable technique to characterize silica-based networks [34]. Such cross-linked structures typically exhibit a number of different silicon environments (labeled Q^0 to Q^4) which give rise to characteristic peaks in their ^{29}Si spectra (δ, ppm) [34]: Q^0 = -66 to -74; Q^1 = -78 to -83; Q^2 = -83 to -88; Q^3 = -90 to -100; Q^4 = -107 to -110. Solid-state ^{29}Si-NMR spectra for all the networks typically showed Q^3- and Q^4-type peaks. For example, DHBA (G0) templated network showed two peaks at -100.7 and 110.5 ppm in its solid-state ^{29}Si spectrum. In addition, DHBA-based networks synthesized using $Si(NMe_2)_4$ reagent showed characteristic peaks between 0 and -30 ppm corresponding to the linkage unit between the dendritic backbone (C_7H_5-$OSiMe_2O$-C_7H_5 or C_7H_5-$OSiMe_2O$-C_6H_3) [19]. The fact that Q^3- and Q^4-type peaks appeared consistently in these networks shows that the networks are composed of dendritic moieties linked to each other by highly cross-linked siloxane bonds [1, 35]. A large number of the bonds in these networks are Si-O-Si bonds instead of Si-O-R bonds (where R = dendrimer's alkyl group). This is the reason that the networks do not collapse upon removal of the templates.

Surface area measurements in these networks were made based on N_2 gas adsorption and desorption by the Brunuauer-Emmett-Teller (BET) method [36-38]. The surface areas for the networks prepared using $Si(NMe_2)_4$ before and after the removal of dendrimer templates are shown in Table 2.1. The surface area of G0-templated network before treatment with HCl to remove the template is very low, and is in fact comparable to the surface area of the network prepared using auto-condensation of $Si(NMe_2)_4$. In contrast, surface areas of the G1-3 templated networks before treatment with HCl are quite high. These results are consistent with the reaction sequence shown in Scheme 2.1 that shows that the network formation takes place around the dendrimer aggregate templates in generations 1-3. Since DHBA does not form any aggregates, its condensation takes place around a very small DHBA molecule, and hence much lower surface area. The networks obtained using G1-3 remain attached to the outer layer of the aggregates while the inner dendrimer molecules leach out upon dilution/washing. As shown in Table 2.1 for G1-3 dendrimer templated networks, in general and as expected, there is an increase in the surface area upon removal of the dendrimer templates by treatment with HCl.

Table 2. 1. BET Surface area measurements for networks prepared using $Si(NMe_2)_4$ before and after removal of dendrimer templates.

Dendrimer templated network	Surface area, before HCl treatment ($m^2.g^{-1}$)	Surface area, after HCl treatment ($m^2.g^{-1}$)
DHBA-G0	9 ± 6	18 ± 10
DHBA-G1	497 ± 26	554 ± 29
DHBA-G2	506 ± 37	791 ± 31
DHBA-G3	421 ± 13	705 ± 39
DHBA-G4	48 ± 5	119 ± 21
DHBA-G5	59 ± 16	41 ± 9
Autocondensation of $Si(NMe_2)_4$	13 ± 10	NA

For G4-5 templated networks, the surface areas are much lower as compared with G1-3 templated networks (Table 2.1). It is known that dendrimers of generations 4 and 5 aggregate to much higher extent and at lower concentrations than generations 1-3 [19-21]. Generations 4 and 5 produce aggregates that are much more globular in shape and much larger in size than those from generations 1-3 dendrimers. Formation of networks takes place around these aggregates through the peripheral OH groups, however, inter-aggregate linking through silica may not be as effective for much larger globular entities as in the case of generations 1-3. This will lead to lower surface area in the resulting networks. In addition, it is also possible that in some of the inter-linked dendrimer-templated networks, aggregated dendrimers get trapped inside, and are not effectively removed upon dilution and even upon treatment with HCl. Since these networks contain higher carbon content, aqueous HCl is not able to penetrate through these networks to cleave the dendrimer-network bond. This was supported by the presence of residual (in some cases, up to 50%) dendritic peaks in the $^{13}C\{^{1}H\}$ NMR of the networks.

2.2.2 TEM Analyses of Templated Networks Prepared Using $Si(NMe_2)_4$

Transmission Electron Microscopy (TEM) has been shown to be a useful technique to visualize micelles, aggregates, and supramolecular entities such as dendrimers [39-41], and we have used it to study morphologies of the dendrimer templated networks described above. The networks were embedded in a polymer matrix using four successive twelve-hour dissolutions in the following ratios of acetone over EPON: 1:1, 1:2, 1:3 and pure EPON. They were then heated at 58 °C for 48 hours, and cut and framed into copper grids prior to their examination under a range of magnifications. One of the important points that is highlighted from the TEM study, is the difference in morphology of networks synthesized using autocondensation of $Si(NMe_2)_4$ and DHBA (G0) templation, with those using dendrimer generations 1-5 as templates. The autocondensation and DHBA (G0) templated networks, in general, showed separated globular structures with an average size of 96 and 140 nm respectively

(Figures 2.2a & b). For dendrimer generation 1-5 based networks (Figure 2.2c & d**)**, larger interconnected structures were formed as highly condensed material. These morphologies of the networks constructed using generations 0-5 dendrimers were retained upon treatment with HCl to remove the templates.

The difference in morphologies of autocondensation and DHBA based networks compared with generation 1-5 templation can be explained considering the evolution of network structure as shown in Scheme 2.1**.** The formation of silica network occurs around a nucleation site, and the condensation process is expected to be dependent on the shape and size of the latter. This, in turn, influences the morphology of the resulting networks, as well as their pore sizes. In autocondensation and DHBA (G0) templated networks, small water or DHBA molecules act as nucleation sites. Due to their small size and the fact that they are flat molecules with a fewer number of hydroxyl groups, the networks can grow only to a limited extent, and the interconnection between two or more growing nucleation sites is less possible. In contrast, generations 1-5 have larger number of hydroxyl groups at the periphery, and form aggregates with an exponential increase in the number of hydroxyl groups on the outside [19-21]. This creates a core with many sites of silica network nucleation around these globular aggregates that allows them to support the growth of larger networks, and offers more opportunities in forming interconnected structures.

The pore sizes in G1-5 templated networks prepared using $Si(NMe_2)_4$ were found to be, on an average, 155, 170, 189, 231, and 255 nm respectively. These values are in agreement with the dendrimer aggregate sizes of G1-5 [19-20]. It has been demonstrated that the larger the dendrimer generation, the larger is the average aggregate. As explained above, since larger aggregates are bigger templates, they would allow a larger core of nucleation sites that can support a larger network with larger pore sizes. The pore sizes of G1-3 templated networks show an increasing pattern, but are close to each other as expected from the corresponding aggregate sizes of the dendrimers, and G4-5 templated networks have larger pore sizes than those of G1-3. These results are in agreement with the BET data presented in Table 2.1, in which bigger hollow spheres in the same volume would give lower surface area than having many smaller spheres in a similar environment.

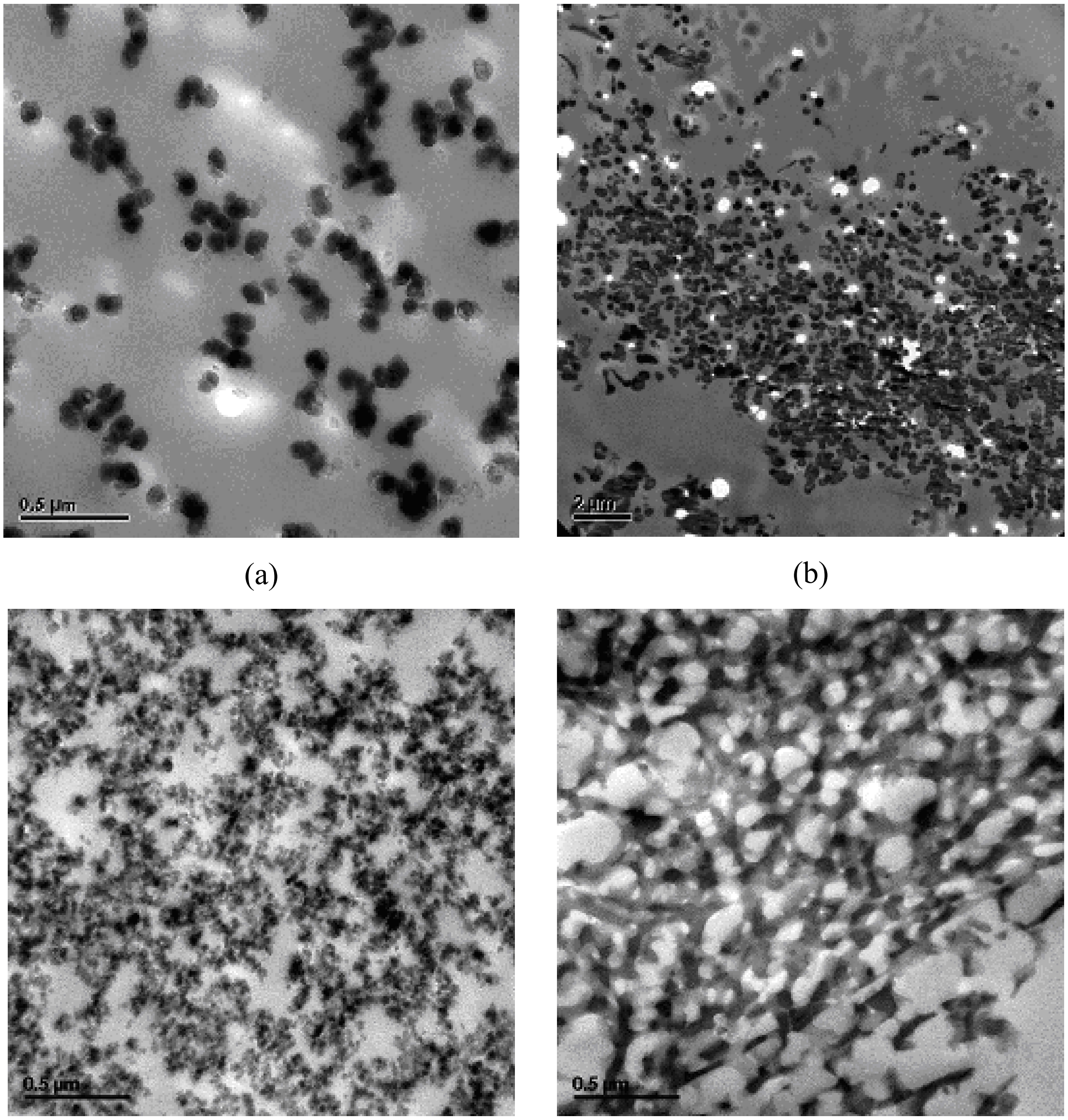

(a) (b)

(c) (d)

Figure 2. 2. Transmission electron microscopy images of the networks prepared using (a) autocondensation; (b) DHBA (G0); (c) dendrimer generation 3 (G3); (d) dendrimer generation 4 (G4).

2.2.3 Dendrimer Templated Networks Prepared Using $ClSi(NEt_2)_3$

We were intrigued upon examination of the solid state $^{13}C\{^1H\}$ NMR spectra of the networks prepared using $ClSi(NEt_2)_3$ which showed no peaks corresponding to DHBA or the dendrimers in their spectra. The FT-IR spectra also depicted the absence of DHBA or dendrimers in the networks. The reaction between the dendrimer OH groups and $ClSi(NEt_2)_3$ produces HCl as well as NEt_2H as by-products. Most of the acid is removed as the salt $NEt_2H.HCl$. However, any residual small amount can act as a catalyst to hydrolyze the alkoxysilane bonds which link the dendrimer templates with the rest of the network. As a result, the dendrimer templates are cleaved *in situ* from the network.

The solid-state $^{13}C\{^1H\}$ NMR spectra for the networks prepared using $ClSi(NEt_2)_3$ displayed only two peaks at δ 13.07 and 43.27 ppm (Figure 2.3a), which can be assigned to ethyl groups on diethylamine substituents in the salt $NEt_2H{\cdot}HCl$. The latter was also confirmed by FT-IR spectra where bands corresponding to the ethylamine group: N-C-H (2821 cm^{-1}), CH_3 (1456 cm^{-1}), CH_2 (1339 cm^{-1}) and the diethylamonium chloride salt ($NEt_2H{\cdot}HCl$): $R_2NH_2^+$ (2969 cm^{-1} region) and $R_2NH_2^+\,{}^-Cl$ salt (1598 cm^{-1}) were observed.

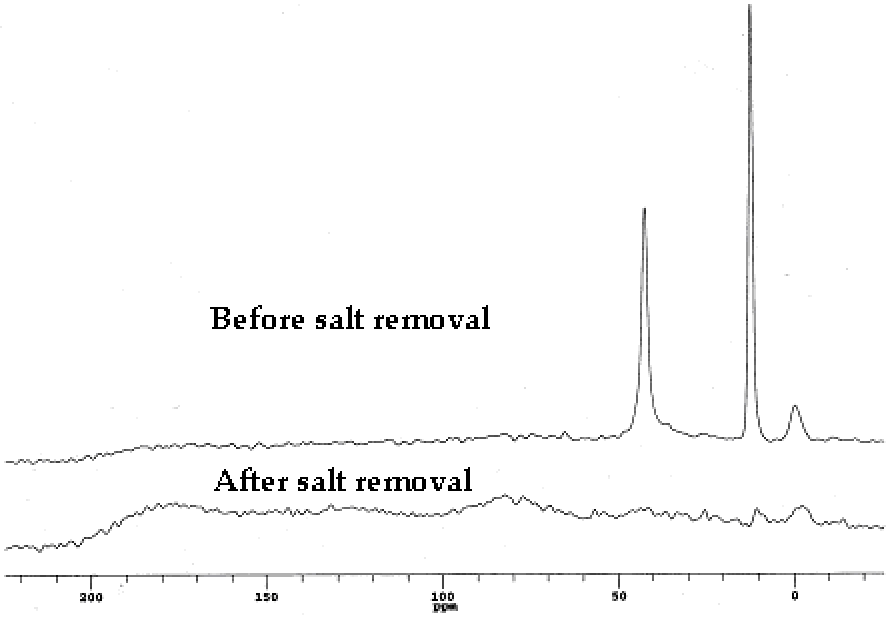

Figure 2. 3. Solid-state $^{13}C\{^1H\}$ NMR spectra of a G0 templated network before (a) and after salt removal (b). The peaks at δ 13.1 and 43.3 ppm correspond to $N(CH_2CH_3)_2H{\cdot}HCl$, and the small peak at 0 ppm is due to grease.

These results show that the diethylamonium salt, which is formed as a by-product in the reaction of dendrimer-OH with $ClSi(NEt_2)_3$, remains trapped in the network even after repeated washings with THF. These results suggest that dendrimer templated networks retain diethylamonium chloride salt inside their cavities after the polycondensation process. THF, that is used as a solvent for these reactions, is not able to penetrate these network materials and access the cavities. In order to remove the trapped diethylamonium chloride salt, we soaked our network materials templated by generations 0-3 dendrimers in water for 15 minutes, and then rinsed with diethyl ether. The analysis of the resulting network by $^{13}C\{^1H\}$ NMR and FT-IR showed that the diethylamonium chloride salt had been removed. The peaks in the $^{13}C\{^1H\}$ NMR spectrum due to $–NEt_2$ had disappeared (Figure 2.3b) and the FT-IR spectra now contained only the bands corresponding to Si-O-Si stretching (broad strong peak at 1088 cm^{-1}) and Si-OH (medium peak at 3399 cm^{-1}). It was noticed that the intensity of bands corresponding to Si-O-Si stretching became much stronger upon removal of the salt. The presence of salt in the networks was also confirmed by weight measurement. After soaking the networks in water, and then washing with diethyl ether and drying, the weight of the sample decreased, and was found to be, in general, equal to one third of the initial weight.

The surface areas of these networks were measured before and after $NEt_2H^{\cdot}HCl$ removal (Table 2.2) and as expected, an increase in surface area was observed upon salt removal. For example, the surface area increased from an average 40 $m^2.g^{-1}$ prior to salt removal, to an average 500 $m^2.g^{-1}$ after its removal. The latter is consistent with the surface area typically found [12,38] in other inorganic-organic hybrid materials.

Table 2. 2. BET Surface area measurements for Networks prepared using $ClSi(NEt_2)_3$ before and after salt removal.

Dendrimer templated network	Surface area, before salt removal ($m^2.g^{-1}$)	Surface area, after salt removal ($m^2.g^{-1}$)
DHBA-G0	42 ± 14	130 ± 53
DHBA-G1	52 ± 14	579 ± 58
DHBA-G2	44 ± 29	541 ± 54
DHBA-G3	48 ± 17	509 ± 51
DHBA-G4	49 ± 17	226 ± 67
DHBA-G5	44 ± 17	388 ± 40
Autocondensation of $ClSi(NEt_2)_3$	62 ± 20	108 ± 38

The surface areas for networks templated with generations 4 and 5 dendrimers were found to be lower upon salt removal as compared to those of generations 1-3 templated networks. This is due to the fact that a relatively large molar equivalence of $ClSi(NEt_2)_3$ was used to synthesize these networks in comparison with the other networks. In these networks large quantities of salt are generated, and rinsing with water does not remove the salt entirely. In fact, solid-state $^{13}C\{^1H\}$-NMR spectra for rinsed G4- and G5-based networks still showed peaks pertaining to residual diethylamine salt though they were considerably much weaker compared to the non-rinsed versions.

The auto-condensation of $ClSi(NEt_2)_3$ to generate a silica network without the use of a template was also carried out for comparison purposes. Its surface area demonstrates the influence which various templates have on the networks as the dendrimer templated networks showed surface areas much larger than the networks prepared from polycondensation of $ClSi(NEt_2)_3$ alone.

2.2.4 TEM Analyses of the Networks Prepared Using $ClSi(NEt_2)_3$

TEM analyses of the networks obtained using $ClSi(NEt_2)_3$ showed very similar results to those obtained above with $Si(NMe_2)_4$. The difference in morphology of networks synthesized using autocondensation and DHBA (G0) with those using dendrimer generations 1-5 was again apparent. The autocondensation and DHBA (G0) templated networks, in general, formed globular structures with an average size of 160 and 200 nm respectively. For generation 1-5 based networks, larger interconnected structures were formed as condensed materials and, in some cases, collapsed networks due to sample preparation, as shown in Figure 2.4 for generation 3 templated networks. Once again, TEM analyses of the dendrimer-templated networks indicated morphologies that were consistent with the proposed condensation methodology shown in Scheme 2.1 in which the construction of the networks takes place around dendrimer aggregates. This phenomenon is also indicative in the synthesis of network structures using other dendritic macromolecules [42].

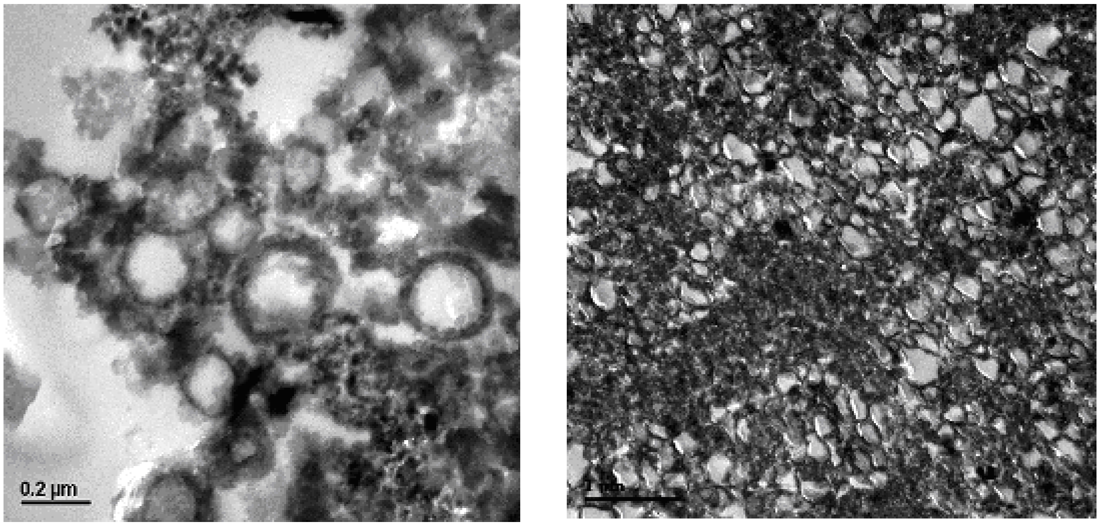

(a) (b)

Figure 2. 4. Transmission electron microscopy images of the networks prepared from $ClSi(NEt_2)_3$ and G3 dendrimer.

The pore sizes in dendrimer generations 1-5 templated networks prepared using $ClSi(NEt_2)_3$ were found to be, on average, 140, 152, 177, 205, and 225 nm. The latter are, once again, in agreement with aggregate sizes of dendrimer generations 1-5 [19-20]. The pore sizes of these networks are slightly lower than those obtained using $Si(NMe_2)_4$. This is expected since, as the dendrimer templates are cleaved *in situ* from the network, the formation of the network could be less uniform, and the templates provide minimal support to a large and dense network construction. In other words, the cleavage of the template while the network is being formed changes the way the network is synthesized around the dendrimer aggregate.

2.2.5 Physical Behavior of the Networks and Encapsulation of Disperse Red 1 (DR1) Dye

We were intrigued to observe that the dendrimer-templated silica networks were water repellent, and upon addition to water had a tendency to float on its surface while sinking in a hydrophobic solvent such as THF. It suggests that the surface of these networks is of a hydrophobic nature whereas the interior is hydrophilic. This might also explain as to why THF was unable to penetrate into the networks synthesized using $ClSi(NEt_2)_3$ and remove $NEt_2H.HCl$ salt.

Disperse red 1 that shows interesting photophysical properties [43,44] with a UV–Vis absorption (λ_{max}) at 485 nm and a red color, is an ideal candidate for exploring molecular encapsulation into the dendrimers templated silica networks described above. Its entrapment into the internal cavities of DHBA-based dendrimers has been examined earlier, in which the dendrimers were placed in a solution of DR1 in THF and an equilibration process led to its inclusion into the dendrimers [19-21]. However, since the silica-based networks are insoluble and display a hydrophobic surface with a hydrophilic interior, a similar process of soaking the networks in solutions of DR1 in THF did not lead to any significant inclusion. We thus developed a new methodology to entrap DR1 into the networks. In a typical experiment, dendrimer templated porous silica was placed in a THF solution of DR1, sonicated for a period of 2h, and the immersed network was then left to stand overnight. The network was filtered, and washed copiously with THF to remove any physisorbed DR1. The network had turned slightly red in color. It was subsequently suspended in light mineral oil, and a thin film of this paste was sandwiched between two quartz slides. The UV-Vis absorption spectra of the latter showed a peak (λ_{max}) at 482 nm, as shown in Figure 2.5, that corresponded well with the UV-Vis absorption behavior for DR1 (λ_{max} at 485 nm). These results clearly suggested that DR1 has been successfully entrapped into the network.

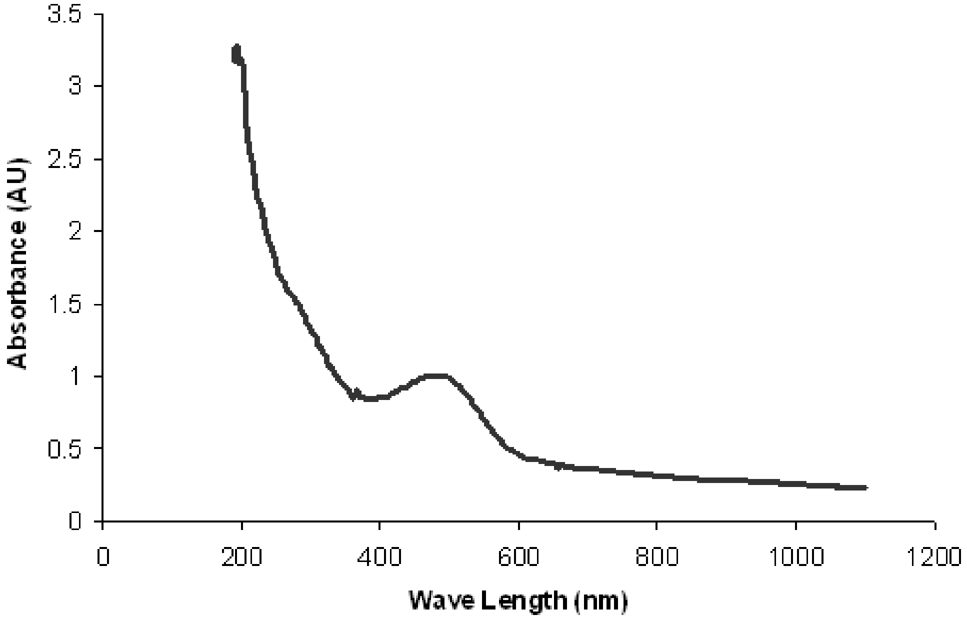

Figure 2. 5. UV-Vis absorption spectrum of the DR1 encapsulated G3 templated network.

2.3 Conclusions

Using a simple sol-gel condensation methodology and easily accessible reagents, we have demonstrated that 3,5-dihydroxybenzyl alcohol (DHBA) based dendrimers of generations 0 to 5 can be used as templates to prepare a variety of interconnected organic – inorganic hybrid networks from which organic moieties are removed *in situ* or upon acid hydrolysis. The former reaction relates to a one-pot synthesis using chlorotris(diethylamino)silane as a coupling reagent that produces hydrochloric acid as a by-product, which helps remove the dendritic moieties from the networks. These network materials retain the diethylamoniumchloride salt (a by-product formed during the reaction) trapped inside the networks, the removal of which leads to significant enhancement of surface areas. There are specific advantages in the selection of the silane reagent employed in the construction of networks with the chlorotris(diethylamino)silane reagent providing a one-pot synthesis, while the tetrakis(dimethylamino)silane yields networks with much higher surface areas. Using transmission electron microscopy, a common globular morphology that becomes denser and more interconnected for higher generations, was observed for materials prepared using generations 1 to 5 dendrimers as templates. A detailed analysis of these networks by a combination of techniques clearly suggests that aggregation, a commonly observed phenomenon that occurs at a relatively low concentration for these types of dendrimers, plays a crucial role in the polycondensation process that leads to network formation around the aggregates and subsequently determines their pore sizes. Dendrimers of generations 1-3 provide a slightly better control on the evolving structure of the networks due to the smaller size of dendritic aggregates compared to those for generations 4-5. Intriguingly, the surface of these network materials was found to be hydrophobic with a hydrophilic interior. This property can be taken advantage of in applications related to molecular drug solubilization, controlled release etc., and we are currently exploring the potential of this phenomenon in more detail. It is demonstrated here that in these networks, molecules such as disperse red 1 can be effectively encapsulated using sonication.

2.4 Experimental Section

All manipulations were performed under a nitrogen atmosphere using either standard Schlenk line techniques or an Innovative Technology (Braun) Labmaster MB-150-M dry box. All dry solvents were stored under nitrogen and used after distillation over sodium. Chemicals were purchased from the following and used as received: 3,5-dihydroxybenzyl alcohol (Aldrich), tetrakis(dimethylamino)silane (Gelest), and silicon tetrachloride (Gelest). ^{1}H NMR spectra were measured on a 270 MHz JEOL spectrometer at ambient temperature. Solution NMR samples were prepared in deuterated solvents (Cambridge Isotope Laboratories, Inc). Solid-state ^{29}Si and ^{13}C{^{1}H} NMR spectra were recorded on a Chemagnetic CMX 300 MHz spectrometer with high-power decoupling. Infrared spectra were measured on a Bruker IFS-48 Fourier transform infrared spectrometer using a standard resolution of 4 cm^{-1} for transmission. Transmission electron microscopy (TEM) investigations were carried out on a JEOL 2000FX microscope operating at an acceleration voltage of 80 kV. Samples analyzed by TEM were prepared after four successive dissolutions of 12h each in acetone / EPON 1:1, 1:2, 1:3, and pure EPON. Then, they were heated at 58°C for 48 hours.

2.4.1 Materials

DHBA based dendrimers were prepared using a procedure described in references 19-21. Chlorotris(diethylamino)silane was prepared as described in reference 45.

2.4.2 Synthesis of Networks Using $Si(NMe_2)_4$

A typical procedure for the synthesis of these networks is described below for G0-dendrimer templated network.

2.4.2.1 G0 Templated Network Using Si(NMe2)4

One equivalent of DHBA (100 mg, 0.714 mmol) was dissolved in 4 ml of dry THF. 3 equivalents (0.5 mL, 2.142 mmol) of $Si(NMe_2)_4$ were added dropwise to the solution. The mixture was stirred at room temperature overnight under nitrogen. It was then brought in contact with air and 2 mL of distilled water were added. The mixture was heated for 10 days at 50 °C. The solution was filtered and a solid material was obtained. Solid-state $^{13}C\{^1H\}$-NMR: δ (ppm) 66.27 (C_6H_3-*C*H_2OSi), 103.2, 109.3 (*C*H from C_6H_3), 142.9 (*C*-CH_2OSi from C_6H_3), 157.1 (*C* –OSi from C_6H_3). Solid-state ^{29}Si-NMR: δ (ppm) –110.0, (C_6H_3-CH_2-O**Si**O-CH_2- C_6H_3) -100.7 (C_6H_3-O**Si**O-CH_2-C_6H_3). FT-IR: ν (cm^{-1}) 666 (Si-O-Si bending), 789 (meta-disubstitution), 959, 1082, 1217 (Si-O stretching), 1628 (C=C), 2815, 2972 (C-H), 3427 (OH) 3745 (Si-OH stretching).

2.4.2.2 G1 Templated Network Using $Si(NMe_2)_4$

The protocol used to prepare this network was identical to that of the reaction of DHBA (G0-templated) with $Si(NMe_2)_4$. Solid-state ^{29}Si NMR: δ (ppm) –17.3

(C_7H_5-O**Si**Me_2O-C_7H_5, C_7H_5-O**Si**Me_2O-C_6H_3), -100.2 (Si Q^3), -110.1 (Si Q^4). Solid-state $^{13}C\{^1H\}$ NMR: δ (ppm) 29.2, 31.4 (C_7H_5-OSiMe_2O-C_7H_5 and C_7H_5-OSiMe_2O-C_6H_3), 67.5 (C_6H_3-*C*H_2OSi), 102.9, 109.2 (*C*H from C_6H_3), 139, 143.3 (*C*-CH_2OSi from C_6H_3), 156.8 (*C* –OSi from C_6H_3). FT-IR: ν (cm^{-1}) 690, 739, 807, 851 (meta-disubstitution; C-H out-of-plane bending), 960, 1095, 1265 (Si-O stretching), 1352, 1402 (alkane C-H bending), 1615, 1467 (aromatic C=C stretching), 2968 (alkane C-H stretching), 3407 [broad] (OH and/or aromatic CH stretching).

2.4.2.3 G2 Templated Network Using $Si(NMe_2)_4$

Solid-state $^{13}C\{^1H\}$-NMR: δ (ppm) 28.3, 25.1 (C_7H_5-OSiMe_2O-C_7H_5 and C_7H_5-OSiMe_2O-C_6H_3), 68 (C_6H_3-*C*H_2OSi), 103, 109 (*C*H from C_6H_3), 143 (*C*-CH_2OSi from C_6H_3), 157 (*C* –OSi from C_6H_3). Solid-state ^{29}Si-NMR: δ (ppm) –16.8 (C_7H_5-O**Si**Me_2O-C_7H_5, C_7H_5-O**Si**Me_2O-C_6H_3), -100.5 (Si Q^3), -109.6 (Si Q^4). FT-IR: ν (cm^{-1}) 558, 452, 699, 808, 849 (meta-disubstitution), 962, 1087, 1163, 1266, 1333 (Si-O stretching), 1602 (C=C), 2969 (C-H), 3382 (OH) 3745 (Si-OH stretching).

2.4.2.4 G3 Templated Network Using $Si(NMe_2)_4$

Solid-state $^{13}C\{^1H\}$-NMR: δ (ppm) 29, 23 (C_7H_5-OSiMe_2O-C_7H_5 and C_7H_5-OSiMe_2O-C_6H_3), 69 (C_6H_3-*C*H_2OSi), 103.1, 109.2 (*C*H from C_6H_3), 139, 143.3 (*C*-CH_2OSi from C_6H_3), 157 (*C* –OSi from C_6H_3). Solid-state ^{29}Si-NMR: δ (ppm) –16.3 (C_7H_5-O**Si**Me_2O-C_7H_5, C_7H_5-O**Si**Me_2O-C_6H_3), -100.3 (Si Q^3), -109.4 (Si Q^4). FT-IR: ν (cm^{-1}) 563, 456, 699, 809, 850 (meta-disubstitution), 960, 1089, 1266 (Si-O stretching), 1632 (C=C), 2968 (C-H), 3441 (OH).

2.4.2.5 G4 Templated Network Using $Si(NMe_2)_4$

Solid-state $^{13}C\{^1H\}$-NMR: δ (ppm) 29.6, 24.7 (C_7H_5-OSiMe_2O-C_7H_5 and C_7H_5-OSiMe_2O-C_6H_3), 66.2 (C_6H_3-*C*H_2OSi), 103.3, 109.2 (*C*H from C_6H_3), 143.0 (*C*-CH_2OSi from C_6H_3), 157.2 (*C* –OSi from C_6H_3). Solid-state ^{29}Si-NMR: δ (ppm) –21.7 (C_7H_5-O**Si**Me_2O-C_7H_5, C_7H_5-O**Si**Me_2O-C_6H_3), -109.1 (Si Q^4). FT-IR: ν (cm^{-1}) 700, 803, 848 (meta-disubstitution), 963, 1099, 1262 (Si-O stretching), 1020, 1151, 1164

(C-O stretching), 1333, 1344, 1491 (alkane C-H bending), 1601 (C=C stretching), 2964 (alkane C-H stretching), 3240, 3379 (OH).

2.4.2.6 G5 Templated Network Using $Si(NMe_2)_4$

Solid-state $^{13}C\{^1H\}$-NMR: δ (ppm) 28.6, 22.7 (C_7H_5-$OSiMe_2O$-C_7H_5 and C_7H_5-$OSiMe_2O$-C_6H_3), 59.5 (C_6H_3-$\mathit{C}H_2OSi$), 108.2, 117.6 (*C*H from C_6H_3), 142.4 (*C*-CH_2OSi from C_6H_3), 158.6 (*C* –OSi from C_6H_3). Solid-state ^{29}Si-NMR: δ (ppm) –21.5 (C_7H_5-O**Si**Me_2O-C_7H_5, C_7H_5-O**Si**Me_2O-C_6H_3), -101.9 (Si Q^3), -109.3 (Si Q^4). FT-IR: ν (cm^{-1}) 700, 803, 848 (meta-disubstitution), 963, 1099, 1262 (Si-O stretching), 1020, 1151, 1164 (C-O stretching), 1333, 1344, 1491 (alkane C-H bending), 1601 (C=C stretching), 2964 (alkane C-H stretching), 3241, 3379 (OH).

2.4.2.7 Removal of Templates

The networks synthesized using $Si(NMe_2)_4$ were suspended in dry THF and stirred overnight at room temperature after the addition of 3 drops of HCl solution (1%). The insoluble powders were filtered and dried. The removal of dendrimers templates was monitored by solid-state $^{13}C\{^1H\}$-NMR and FT-IR that showed the disappearance of the peaks assigned to dendrimers backbone.

2.4.2.8 Autocondensation of $Si(NMe_2)_4$

0.687 mL (2.942 mmol) of $Si(NMe_2)_4$ were added to 10 ml of THF. After stirring overnight, the solution was exposed to air and heated at 57°C for 3.5 months. During this time a precipitate appeared. The solution was filtrated and the solid was air-dried. Solid-state ^{29}Si NMR: -17.6, -22.2 (strong peaks; C_7H_5-O**Si**Me_2O-C_7H_5, C_7H_5-O**Si**Me_2O-C_6H_3), from ~ -100.0 to -108.5 (weak peaks; Si Q^3 and Q^4). FT-IR: ν (cm^{-1}) 803, 851 (Si-N stretching, strong peaks), 1027, 1096 (Si-O stretching; strong & broad peaks), 1262 (Si-CH_3 stretching, strong & sharp peak), 1347, 1407 (C-H scissoring & bending), 1383 (CH_3 umbrella deformation), 1628 (N-H bending, medium), 2965 (alkane C-H stretching), 3427 [broad] (OH stretching).

2.4.2.9 Autocondensation of $ClSi(NEt_2)_3$

100 mg of $ClSi(NEt_2)_3$ were added to 10 ml of THF. After stirring overnight, the solution was exposed to air and heated at 55°C for 72 hours. The solution was filtrated and the solid dried under vacuum. $^{13}C\{^1H\}$ NMR: δ (ppm) 13.1, 43.2 (CH_3-CH_2-N). Solid-state ^{29}Si NMR: δ (ppm) –108.8 (Si Q^4), -100.8 (Si Q^3). FT-IR: ν (cm^{-1}) 3470 (OH), 1156, 1076 (Si-O stretching). FT-IR: ν (cm^{-1}) 3470 (OH), 1158, 1059 (Si-O stretching), 848 (SiOH), 2969 ($R_2NH_2^+$), 2821, 2774 (N-C-H), 1598 ($R_2NH_2^{+-}Cl$), 1456 (CH_3), 1398 (CH_2).

2.4.3 Synthesis of Networks Using $ClSi(NEt_2)_3$

A typical procedure for the synthesis of these networks is described below for G0-dendrimer templated network.

2.4.3.1 G0 Templated Network Using $ClSi(NEt_2)_3$

One equivalent of 3,5-dihydroxybenzyl alcohol (200 mg, 1.429 mmol) was dissolved in 10 mL of dry THF. 3 equivalents of chlorotris(diethylamino)silane (4.287 mmol) were added dropwise to the solution. The mixture was stirred at room temperature overnight. It was removed from the nitrogen atmosphere and exposed to air, and left for 72 h at 58 °C. The solution was filtrated, and the solid was dried under vacuum. Solid-state $^{13}C\{^1H\}$ NMR: δ (ppm) 13.07, 43.3 (CH_3-CH_2-N). Solid-state ^{29}Si NMR: δ (ppm) –109.4 (Si Q^4), -100.8 (Si Q^3). FT-IR: ν (cm^{-1}) 3470 (OH), 1159, 1052 (Si-O stretching), 848 (SiOH), no peaks corresponding to CH aromatic, 2969 ($R_2NH_2^+$), 2821, 2774 (N-C-H), 1598 ($R_2NH_2^{+-}Cl$), 1456 (CH_3), 1398 (CH_2).

2.4.3.2 G1 Templated Network Using $ClSi(NEt_2)_3$

Solid-state $^{13}C\{^1H\}$ NMR: δ (ppm) 12.9, 44.1 (CH_3-CH_2-N). Solid-state ^{29}Si NMR δ (ppm) –109.2 (Si Q^4), -100 (Si Q^3). FT-IR: ν (cm^{-1}) 3470 (OH), 1158, 1059 (Si-O stretching), 848 (SiOH), no peaks corresponding to CH aromatic, 2969 ($R_2NH_2^+$), 2821, 2774 (N-C-H), 1598 ($R_2NH_2^{+-}Cl$), 1456 (CH_3), 1398 (CH_2).

2.4.3.3 G2 Templated Network Using $ClSi(NEt_2)_3$

Solid-state $^{13}C\{^1H\}$ NMR: δ (ppm) 13.0, 43.3 (CH_3-CH_2-N). Solid-state ^{29}Si NMR: δ (ppm) –108.2 (Si Q^4), -100.3 (Si Q^3). FT-IR: ν (cm^{-1}) 3470 (OH), 1158, 1059 (Si-O stretching), 848 (SiOH), no peaks corresponding to CH aromatic, 2969 ($R_2NH_2^+$), 2821, 2774 (N-C-H), 1598 ($R_2NH_2^{+-}Cl$), 1456 (CH_3), 1398 (CH_2).

2.4.3.4 G3 Templated Network Using $ClSi(NEt_2)_3$

Solid-state $^{13}C\{^1H\}$ NMR: δ (ppm) 13.1, 43 (CH_3-CH_2-N). Solid-state ^{29}Si NMR: δ (ppm) –109 (Si Q^4), -101.3 (Si Q^3). FT-IR: 3470 (OH), 1158, 1059 (Si-O stretching), 848 (SiOH), no peaks corresponding to CH aromatic, 2969 ($R_2NH_2^+$), 2821, 2774 (N-C-H), 1598 ($R_2NH_2^{+-}Cl$), 1456 (CH_3), 1398 (CH_2).

2.4.3.5 G4 Templated Network Using $ClSi(NEt_2)_3$

Solid-state $^{13}C\{^1H\}$ NMR: δ (ppm) 13.07, 43.27 (CH_3-CH_2-N). Solid-state ^{29}Si NMR: δ (ppm) –109.4, (Si Q^4), -100.8 (Si Q^3). FT-IR: ν (cm^{-1}) 3470 (OH), 1158, 1059 (Si-O stretching), 848 (SiOH), no peaks corresponding to CH aromatic, 2969 ($R_2NH_2^+$), 2821, 2774 (N-C-H), 1598 ($R_2NH_2^{+-}Cl$), 1456 (CH_3), 1398 (CH_2).

2.4.3.6 G5 Templated Network Using $ClSi(NEt_2)_3$

Solid-state $^{13}C\{^1H\}$ NMR: δ (ppm) 13.4, 43.6 (CH_3-CH_2-N). Solid-state ^{29}Si NMR: δ (ppm) –108.5, (Si Q^4), -101.0 (Si Q^3), -14.9. FT-IR: ν (cm^{-1}) 3470 (OH), 1158, 1059 (Si-O stretching), 848 (SiOH), no peaks corresponding to CH aromatic, 2969 ($R_2NH_2^+$), 2821, 2774 (N-C-H), 1598 ($R_2NH_2^{+-}Cl$), 1456 (CH_3), 1398 (CH_2).

2.4.3.7 Removal of $NEt_2H.HCl$ Salt

The networks prepared using $ClSi(NEt_2)_3$ were soaked in water, and after 15 minutes of stirring were washed with diethyl ether. Then they were put in the oven at 120°C for 1 hour. Solid-state $^{13}C\{^1H\}$ NMR: δ (ppm): no peaks. FT-IR: ν (cm^{-1}) 3399

(OH), 1088 (broad strong peak, Si-O stretching), 798 (SiOH).

2.5 Acknowledgements

We would like to thank NSERC of Canada, FQRNT (Quebec, Canada), and the Centre for Self-Assembled Chemical Structures (FQRNT) for financial assistance.

References

1. F. Hof, S. L. Craig, C. Nuckolls and J. Rubek, *Angew. Chem. Int. Ed. Engl.*, 2002, **41**, 1488.
2. C.-Y. Su, M. D. Smith and H.-C. Loyle, *Angew. Chem., Int. Ed. Engl.*, 2003, **42**, 4085.
3. C.-Y. Lai, B. G. Treyn, D. M. Jeftinija, K. Jeftinija, S. Xu and V. S.-Y. Lin, *J. Am. Chem. Soc.*, 2003, **125**, 4451.
4. L. R. Nassimbeni, *Acc. Chem. Res.*, 2003, **36**, 631.
5. C. T. Kresge, M.E. Leonowicz, W. J. Roth, J. C. Vartuli and J. S. Beck, *Nature*, 1992, **359**,710.
6. J. S. Beck and J. C. Vartuli, *Curr. Opinion in Solid State and Materials Science*, 1996, **1**, 76.
7. M. Fisher and F. Vogtle, *Angew. Chem. Int. Ed. Engl.*, 1999, **38**, 884.
8. A. K. Patri, I. J. Majoros and J. R. Baker Jr., *Current Opinion in Chemical Biology*, 2002, **6**, 466.
9. G. R. Newkome, E. He and C.N. Moorefield, *Chem. Rev.* 1999, **99 (7)**, 1689.
10. M. R. Knecht, S. L. Sewell and D.W. Wright, *Langmuir*, 2005, **21**, 2058.
11. P. R. Dvornic, J. Li, A. M. Leuze-Jallouli (de), S. D. Reeves and M. J. Owen, *Macromolecules*, 2002, **35**, 9323.
12. P. R. Dvornic, J. Hu, S. D. Reeves and M. J. Owen, *Silicon Chemistry*, 2002, **1**, 177.
13. S. Jahromi and B. Mostert, *Macromolecules*, 2004, **37**, 2159.
14. J. W. Kriesel and T. D. Tilley, *Chem. Mater.* 1999, **11**, 1190.
15. G. J. A. A. Soler-Illia, L. Rozes, M. K. Boggiano, C. Sanchez, C.-O. Turrin, A.-M. Caminade and J.-P. Majoral, *Angew. Chem. Int. Ed.*, 2000, **39**, 4249.
16. G. Larsen, E. Lotero and M. Marquez, *Chem. Mater.*, 2000, **12**, 1513.
17. H. Zeng, G. R. Newkome and C. L. Hill, *Angew. Chem., Int. Ed.*, 2000, **39**, 1771.
18. C. O. Turrin, V. Maraval, A.-M. Caminade, J. P. Majoral, A. Mehdi and C. Rey´e, *Chem. Mater.*, 2000, **12**, 3848.
19. O. Bourrier and A. K. Kakkar, *J. Mater. Chem***.,** 2003**,** **13**, 1306.

20. O. Bourrier, J. Butlin, R. Hourani and A. K. Kakkar, *Inorg. Chim. Acta.*, 2004**, 357**, 3836.
21. R. Hourani, M. A. Whitehead and A. K. Kakkar, *J. Mater. Chem*., 2005**, 15**, 2106.
22. F. Chaumel, H. Jiang and A. K. Kakkar*,* A., *Chem. Mater.*, 2001, **13**, 3389.
23. H. Jiang and A. K. Kakkar, *J. Am. Chem. Soc.*, 1999, **121**, 3657.
24. H. Maeda, L. W. Seymour and Y. Miyamoto, *Bioconjugate Chem.*, 1992, **3**, 351.
25. G. Teobaldi and F. Zerbetto, *J. Am. Chem. Soc.*, 2003, **125**, 7388.
26. M. Liu and J.-M.J. Fréchet, *Pharm. Sci. Technol. Today*, 1999, **2**, 393.
27. M. Liu, K. Kono and J.-M.J. Fréchet, *J. Polym. Sci., Polym. Chem.*, 1999, **37**, 3492.
28. K. Kono, M. Liu and J.-M. J. Fréchet, *Bioconjugate Chem.*, 1999, **10**, 1115.
29. S. M. Grayson, M. Jayaraman and J.-M. J. Fréchet, *Chem. Comm*., 1999, **14**, 1329.
30. R. Esfand and D. A. Tomalia, *Drug Discovery Today*, 2001, **6**, 427.
31. W. Ong, A. E. Kaifer, *Angew. Chem. Int. Ed.*, 2003, **42**, 2164.
32. M. G. L. Petrucci, V. Guillemette, M. Dasgupta and A. K. Kakkar, *J. Am. Chem. Soc.*, 1999**, 121,** 1968.
33. M. Dasgupta, B. Peori and A. K. Kakkar, *Coord. Chem. Rev*., 2002, **223**, 233.
34. R. H. Glaser, G. L. Wilkes and C. E. Bronnimann, C. E., *Journal of Non-Crystalline Solids*, 1989, **113**, 73.
35. Q. Zhang, K. Ariga, A. Okabe and T. Aida, *J. Am. Chem. Soc.*, 2004, **126**, 988.
36. J. Retuert, R. Quijada and V. Arias, *Journal of Material Research*, 2003, **18**, 487.
37. L. D. Gelb and K. E. Gubbins, *Langmuir*, 1998, **14**, 2097.
38. S. A. Johnsen, P. J. Olivier, T.E. Mallouk, *Science*, 1998, **283**, 963.
39. C. T. Kresge, M. E. Leonowicz, W. J. Roth, J. C. Vartuli and J. S. Beck, *Nature*, 1992, **359**, 710.
40. S. D. Hudson, H. T. Jung, V. Percec, W. D. Cho, G. Johanssonn, G. Ungar and V. S. K. Balagurusamy, *Science*, 1997, **278**, 449.
41. Percec, V.; Ahn, C.H.; Ungart, G.; Yeardley, D. J. P.; Möller, M.; Sheiko, S. S. *Nature* **1998**, *391*, 161.
42. A. Bouchara, L. Rozes, G. J. De A. A. Soler-Illia, C. Sanchez, C.-O. Turrin, A.-M. Caminade and J.-P. Majoral, *Journal of Sol-Gel Science and Technology*, 2003, **26**, 629.

43. G. Iftime, L. Fisher, A. Natansohn and P. Rochon, *Can. J. Chem.*, 2000, **78**, 409.

44. B. Paci, C. Schmidt, C. Fiorini, J.-M. Nunzi, C. Arbez-Gindre and C.G. Screttas, *J. Chem. Phys.*, 1999, **111**, *16*, 7486

45. F. Chaumel, *A New Synthetic Route to Sol-Gel Materials Containing Nonlinear Optical Chromophores*, **2001**, M.Sc. Thesis, McGill University.

Chapter 3:

Part 1: Overview of Silver Nanoparticles.

Part 2: Tailoring Silver Nanoparticle Construction Using Dendrimer Templated Silica Networks.

(Submitted to *Nanotechnology*, 2008)

Part 1: Overview of silver nanoparticles

Nanoscience has blossomed over the years, and nanotechnology has become more important in many areas including computing, sensors, biomedical applications, etc [1]. Metallic nanoparticles of gold, platinum, palladium, which exhibit unusual optical, thermal, chemical, and physical properties, are of particular interest in terms of their synthesis and evaluation of their properties, because of the promising applications as catalysts, ferrofluids and semiconductors [2, 3]. The investigation of metallic nanoparticles is focused more specifically on their size-dependent characteristic properties, which lead to unique optical, electrical, catalytic, and magnetic behaviours. Much effort has been spent on synthesizing nanoparticles of various metals, sizes, and shapes, as well as to efficiently assemble them into complex architectures [3-5]. Among these metals, silver, in particular, has the highest electrical and thermal conductivity and the unique optical properties, as well as being a catalyst, making it the most attractive metal for a variety of applications in many areas [6]. The control of its properties and applications can be fairly established by changing the size of silver particle to nanometer regime, leading to size and shape dependent chemical, electrical, mechanical, and optical properties [6]. The size and shape of silver nanoparticles can be generally controlled by variation of synthetic procedures [7].

3.1.1 Preparation of silver nanoparticles

The synthesis of particles of submicron or nanosize dimensions has been attempted for centuries [1]. For noble-metal nanoparticles, an effective synthetic technique is required to control the shapes and sizes of nanoparticles. Here two main aspects have been focused on: one is the controllable growth of metal nanoparticles in terms of particle size, size distribution, and structure of the particles. The other is the stabilization of colloids. The usual method for making such metal nanoparticles involves chemical or physical reduction of metal ions in the presence of protective agents, which prevents the nanoparticles from aggregation. By using various reductants, stabilizers and solvents, one can prepare metal nanoparticles with the desired control of particle size and morphologies. To prepare silver nanoparticles, many methods have been reported in literature. Zhang *et al* [7] has provided a review of these methods, that include chemical reduction and photoinduced reduction. Chemical reduction, the most common method, has been extensively investigated in the preparation of silver nanoparticels because of the production of large quantities of nanoparticles in relatively short period of time, under simple and mild reaction conditions.

3.1.1.1 Chemical reduction method

Named as Lee-Meisel method, the earliest, most common and solution-phase synthetic technique for preparation of silver nanoparticles, is the reduction of silver nitrate ($AgNO_3$) with sodium borohydride ($NaBH_4$) [1]. After various modifications of Lee-Meisel method, series of silver salts, such as silver perchlorate ($AgClO_4$) [8], silver tetrafluoroborate ($AgBF_4$) [9], $[Ag(NH_3)_2]NO_3$ [10], and silver acetate (CH_3COOAg) [11], and chemical reducing agents, such as polyol (ethylene glycol, polyvinylpyrrolidone (PVP)) [6], N_2H_4, NH_2OH, $(CH_3)_2NHBH_3$, ethanol, citrate, formamide, formaldehyde, Tollen's reagents, ascorbic acid , and polyaniline or o-anisidine [2], have been utilized for the synthesis of silver suspensions in aqueous solutions or non-aqueous solutions. For example, Leopold *et al* [12] produced highly sensitive silver colloids for surface-enhanced Raman scattering (SERS) by using silver nitrate with hydroxylamine hydrochloride in aqueous solution, at alkaline pH and room temperature within a short time. By changing the mixing order and rate of the two involved solutions, the size and dispersion of silver colloids can be controlled. Pastoriza-Santos et al [13] synthesized polygonal (mainly triangular) silver nanoprisms by boiling $AgNO_3$ in *N*,*N*-dimethyl formamide (DMF), in the presence of poly(vinylpyrrolidone). These kinds of nanoprisms are also stable in other solvents, such as ethanol and water, and solvent exchange leads to strong shifts of the in-plane dipole plasmon band.

Different shapes of silver nanoparticles can be obtained by controlling the reaction conditions of chemical reduction. However, the aggregation of silver nanoparticles may result in the loss of characteristic properties [7]. For low ionic strength aqueous and alcoholic suspension, the thick electrical double layers around silver nanoparticles can prevent the aggregation of silver nanoparticles, but for the high ionic strength or organic-phase suspension, the most important key is to avoid the agglomeration of silver nanoparticles during the synthesis and preservation procedures [1]. Thus, compounds such as surfactants [14, 15], polymers [2, 16-18], stabilizing ligands [7], and dendrimers [19, 20], are used as the protective agents to inhibit the coalescence of silver nanoparticles. The choice of particular protective agent becomes one of the most important factors in the preparation of silver nanoparticles.

3.1.1.2 Physical reduction method

Compared with traditional chemical reduction methods, techniques such as microwave-assisted [21, 22], irradiation induction [4, 5, 23-25], ultrasonic-assisted [26, 27], photoinducted [28], and electrolysis [29] have also been used in the synthesis of silver nanoparticles. These new methods provide the possibility of control of particle size and then potential for practical applications of the silver nanoparticles. For example, microwaves are widely used in synthetic chemistry because they are fast, simple and efficient in energy supply. Their rapid and uniform heating and consequent dramatic increase in reaction rate can make microwaves useful in the preparation of silver nanoparticles [22]. Patel *et al* [21] used microwave dielectric heating to synthesize nanosize silver particles in three different solvents, water, ethylene glycol, and glycerol, getting the average particle size between 15 and 30 nm. Laser ablation is also a useful technique in the rapid and simple synthesis of silver nanoparticles with highly reproducible properties. Some researchers have investigated the influence of laser ablation on the synthesis of silver nanoparticles [4]. The wavelength of laser light significantly affects the ablation efficiency. It is still not very clear about the influence of laser ablation to the particle size distributions. However, Stietz's experimental results showed that this method can apply to narrow particle size distributions by more than 60% [24]. Sonochemical method has been used for some time since it was discovered as early as 1934 [26]. Sonochemistry arises from acoustic cavitation growth, and implosive collapse of bubbles in a liquid [30]. The collapse of bubbles generates localized hot spots with very high transient temperatures and pressures. Volatile organometallic compounds inside the cavitating bubble are decomposed to yield individual metal atoms, resulting in narrow particle size distributions.

3.1.1.3 Template synthesis of silver nanoparticles

The ordered mesoporous silica materials with various pore size and structures have attracted a great interest in the application of the synthesis of metallic nanoparticles. By using mesoporous silica such as FSM-16, MCM-14, SBA-15 as templates, it is possible to better control the size and shape of nanoparticles [31-33]. Among various preparation methods of silver nanoparticles, template synthesis became one of the promising methods, in which mesoporous silica materials are used as a host to confine silver nanoparticles as a guest. The basic principle for template synthesis is impregnation of mesoporous silica host matrices with silver ion solutions. The formation of nanoparticles inside the pore is achieved through subsequent chemical reduction or thermal and other treatments. This leads to nanoparticles with a size and shape that is directly related to the initial pore structure of mesoporous silica materials. Among these, Armelao *et al* [11] prepared mesoporous silica materials by a sol-gel procedure using TEOS as silica source and surfactant polyethylene glycol octadecyl ether [Brij76, $CH_3(CH_2)_{16}CH_2(OCH_2CH_2)_{10}OH$] as the structure-directing agent. Ag-SO_2 nanocomposites were obtained by metallation of the mesoporous silica powder with aqueous solutions of silver acetate. The XRD results showed the formation of silver nanoparticles, which were also confirmed by the TEM analysis. Ramnani et al [34] synthesized silver nanoparticles on silica aerogel by using gamma radiolysis. The synthesis starts directly with the addition of silver ion solutions into the aqueous silica aerogel suspension, followed by gamma radiation. The formation of silver clusters was characterized using XRPD, UV, and TEM.

3.1.2 Characterization of silver nanoparticles

The common methods which are used to characterize silver nanoparticles are Transmission Electron Microscopy (TEM), UV-Visible spectroscopy, and X-Ray Powder Diffraction (XRPD). The principles of these techniques have already been introduced in Chapter one. In general, TEM samples are prepared by dropping the silver suspension onto a standard carbon-coated copper grid and drying it in air at room temperature. The size distributions are measured by counting the individual images from different parts of grid. The number average radius can be given by the analysis of hundreds of particles. For UV-visible spectroscopy, absorption bands of the UV-visible spectra can be used to provide information on particle size. The position, which is generally located in the range of 410 to 450 nm, and magnitude of the absorption band are strongly dependent on the size of the particles. As the size decreases, the peak shifts slightly to higher energies [35]. In XRPD, the peaks of silver nanoparticles are generally located at 2θ = 38.1°, 44.3°, 64.4°, and 77.3°, attributed to the (111), (200), (220), and (311) reflection of *fcc* crystalline silver, respectively [11].

References

1. D. D. Evanoff Jr and G.Chumanov, *ChemPhysChem*, 2005. **6**(7): p. 1221-1231.
2. Y. Tan, X. Dai, Y. Li and D. Zhu, *J. Mater. Chem.*, 2003. **13**(5): p. 1069-1075.
3. K. K. Caswell, C. M. Bender and C. J. Murphy, *Nano Letters*, 2003. **3**(5): p. 667-669.
4. F. Mafune, J. Y. Kohno, Y. Takeda, T. Kondow and H. Sawabe, *J. Phys. Chem. B*, 2000. **104**(35): p. 8333-8337.
5. L. Yang, Y. Shen, A. Xie, B. Zhang, *J. Phys. Chem. C*, 2007. **111**(14): p. 5300-5308.
6. B. Wiley, Y. Sun and Y. Xia, *Acc. Chem. Res.,* 2007. **40**(10): p. 1067-1076.
7. W. Zhang, X. Qiao and J. Chen, *Mater. Sci. and Eng.: B*, 2007. **142**(1): p. 1-15.
8. S. Sato, N. Asai and M. Yonese, *Colloid & Polymer Science,* 1996. **274**(9): p. 889-893.
9. Y. W. Kim, D. K. Lee, K. J. Lee, B. R. Min and J. H. Kim, *J. Polym. Sci.: Part B: Polymer Physics*. 2007. **45**(11): p. 1283-1290.
10. Y. Plyuto, J.-M. Berquier, C. Jacquiod and C. Ricolleau, *Chem. Comm.*, 1999. **17**: p. 1653 - 1654.
11. L. Armelao, G. Bottaro, R. Campostrini, S. Gialanella, M. Ischia, F. Poli and E. Tondello, *Nanotechnology*, 2007. **18**: p. 155606.
12. N. Leopold, and B. Lendl, *J. Phys. Chem. B*, 2003. **107**(24): p. 5723-5727.
13. I. Pastoriza-Santos and L.M. Liz-Marzan, *Nano Letters*, 2002. **2**(8): p. 903-905.
14. I. Sondi, D.V. Goia and E. Matijevic, *Journal of Colloid and Interface Science,* 2003. **260**(1): p. 75-81.
15. J. P. Cason, K. Khambaswadkar and C.B. Roberts, *Industrial & Engineering Chemistry Research*, 2000. **39**(12): p. 4749-4755.
16. K. P. Velikov, G. E. Zegers and A. van Blaaderen, *Langmuir*, 2003. **19**(4): p. 1384-1389.
17. R. He, X. Qian, J. Yin and Z. Zhu, *J. Mater. Chem.*, 2002. **12**(12): p. 3783-3786.
18. D.-H.Chen and Y.-W. Huang, *Journal of Colloid and Interface Science*, 2002. **255**(2): p. 299-302.
19. K. Esumi, A. Suzuki, A. Yamahira and K. Torigoe, *Langmuir*, 2000. **16**(6): p. 2604-2608.

20. R. M. Crooks, M. Zhao, L. Sun, V. Chechik and L. K. Yeung, *Acc. Chem. Res.,* 2001. **34**(3): p. 181-190.
21. K. Patel, S. Kapoor, D. Dave, T. Mukherjee, *J. Chem. Sci.,* 2005. **117**(1): p. 53-60.
22. B. He, J. J. Tan, K. Y. Liew and H. Liu, *Journal of Molecular Catalysis A: Chemical,* 2004. **221**(1-2): p. 121-126.
23. K. A. Bogle, S. D. Dhole and V. N. Bhoraskar, *Nanotechnology*, 2006. **17**: p. 3204-3208.
24. F. Stietz, *Applied Physics A: Materials Science & Processing,* 2001. **72**(4): p. 381.
25. J. P. Abid, A. W. Wark, P. F. Brevet and H. H. Girault, *Chem. Comm.,* 2002(7): p. 792-793.
26. J. Zhu, S. Liu, O. Palchik, Y. Koltypin and A. Gedanken, *Langmuir,* 2000. **16**(16): p. 6396-6399.
27. Y. Socol, O. Abramson, A. Gedanken, Y. Meshorer, L. Berenstein and A. Zaban, *Langmuir*, 2002. **18**(12): p. 4736-4740.
28. Q. F. Zhou and Z. Xu, *J. Mater. Scien.,* 2004. **39**(7): p. 2487-2491.
29. N. A. Kotov, M. E. D. Zaniquelli, F. C. Meldrum and J. H. Fendler, *Langmuir*, 1993. **9**(12).
30. K. S. Suslick, M. Fang and T. Hyeon, *J. the Ame. Chem. Soci.*, 1996. **118**(47): p. 11960-11961.
31. A. Fukuoka, H. Araki, J.-ichi Kimura, Y. Sakamoto, T. Higuchi, N. Sugimoto, S. Inagaki and M. Ichikawa, *J. Mater. Chem.*, 2004. **14**: p. 752 - 756.
32. T. Gacoin, S. Besson and J. P. Boilot., *J. Phys.: Condens. Matter*, 2006. **18**: p. S85-S95.
33. J.-L. Shi, Z.-L. Hua and L.-X. Zhang, *J. Mater. Chem.,* 2004. **14**(5): p. 795-806.
34. S. P. Ramnani, J. Biswal and S. Sabharwal, *Radiation Physics and Chemistry*, 2007. **76**(8-9): p. 1290-1294.
35. Y. Tan, Y. Wang, L. Jiang, D. Zhu, *Journal of Colloid and Interface Science*, 2002. **249**(2): p. 336-345.

Part 2: Tailoring Silver Nanoparticle Construction Using Dendrimer Templated Silica Networks

3.2.1 Introduction

Metal nanoparticles continue to attract interest of scientists from all disciplines due to their unique properties that lend themselves to widespread applications in a variety of areas including optoelectronics, catalysis, sensing, and biomedical applications [1]. Among this elevated activity, designing new pathways to synthesize silver nanoparticles has also gained much attention, and several methodologies have been developed in which a metal salt is reduced under a variety of stabilizing environments [2]. Silica based networks have also offered one of these platforms since their internal structure can be tailored, which can then be utilized to control location of the metal particles [3]. We have recently reported a simple methodology in which 3,5-dihydroxybenzyl alcohol (DHBA) based dendrimers [4] were used as templates in the construction of silica based networks [5]. These networks contain Si-OH groups directed inwards, as indicated by their water-repellent behavior on the surface. We were intrigued by taking advantage of these internal acidic sites and explore their potential in constructing nanoparticles, and examine the role of residual dendrimer in the synthesis of metal particles. In this manuscript, we report a methodology in which silver metal ions are chemisorbed into the silica networks, followed by nanoparticle build-up based on the type of network employed for their synthesis. A detailed characterization using a variety of techniques including UV-Vis spectroscopy, X-ray powder diffraction and transmission electron microscopy demonstrates that the metal particle growth is influenced by the network, and those templated from dendrimer generations 1-3 and from which dendrimer is completely removed, lead to the formation of Ag_2O particles, while the network prepared using dendrimer generation 4 as the template, and in which there is residual dendrimer, yield silver nanoparticles exclusively without requiring any external reducing agent.

3. 2.2 Experimental Details

3.2.2.1 Materials and Methods

3,5-dihydroxybenzyl alcohol (DHBA) and silver acetate were purchased from Aldrich, and were used as received. DHBA-based dendrimers and the corresponding dendrimer-templated silica networks were synthesized using a procedure as described in references [4c-e] and [5]. Solid-state $^{13}C\{^1H\}$ NMR spectra were obtained on Chemagnetic CMX 300 MHz spectrometer with high-power decoupling. UV-Vis measurements were carried out in water on a Hewlett Packard 8453 with a resolution of 2 nm. Transmission electron microscopy measurements were performed on a JEOL 2000FX microscope operating at an acceleration voltage of 80 kV. X-ray powder diffraction experiments were performed using a Siemens D-5000 diffractometer, equipped with a step scanner and a 1.2 kW cobalt tube (λ=1.5406 Å) coupled to a silicon detector. The diffraction patterns were acquired in the reflection mode, for 2θ values ranging from 4 to 90 degrees. The X-ray beam was fixed while the sample holder and the detector were moved to scan the solids.

3.2.2.2 Synthesis of Metal Particles Using G1-3 Dendrimer Templated Silica Networks

In a typical procedure, 50 mg of the network were added to 12 mL of an aqueous solution of silver acetate (10^{-2}M), and stirred for one week. The networks floated on top of the solution, and no mixing was observed. Solvent was then removed on a rotary evaporator at 40 ˚C, and the residue was rinsed with water, filtered and vacuum dried to yield light brown (G1-network) to dark brown (G2-3 networks) solids.

3.2.2.3 Synthesis of Metal Particles Using G4 Dendrimer Templated Silica Network

55 mg of G4 network were added to 12 mL of an aqueous solution of silver acetate (10^{-2}M), and stirred for an hour at room temperature. The color changed quickly

to green, and a typical intense smell of acetic acid was noticed. The solvent was then removed on a rotary evaporator at 40 ˚C, and the residue was rinsed with water, filtered under vacuum, and upon drying yielded a dark solid.

3.2.3 Results and discussion

Silver metal nanoparticles were constructed using silica networks that were synthesized by employing 3,5-dihydroxybenzyl alcohol (DHBA) based dendrimers as templates. A detailed synthesis and characterization of dendrimers, and the corresponding silica networks has been reported earlier [4c-e, 5]. We have also demonstrated that these networks are water repellent on their surface, and this behavior is prominent in networks in which the template has been completely and effectively removed. For the work reported here, we chose generations 1-3 dendrimer templated networks from which dendrimer was completely removed from the network, and generation 4 templated network that had residual dendrimer in it.

In a typical reaction used for the synthesis of silver particles, 50 mg of the network were added to a 12 mL aqueous solution (10^{-2}M) of silver acetate, and the mixture was stirred at room temperature. The networks synthesized using generations 1-3 dendrimers (G1-3) floated on the surface of aqueous silver acetate solution (Figure 3.1a), and even vigorous stirring did not lead to any significant wetting of the solid. After stirring over a period of about one week, slow removal of the solvent was carried out on a rotary evaporator at 40 ˚C. The resulting solids were rinsed with water to remove any residual silver acetate, and upon filtration under vacuum led to the isolation of light to dark brown (G1-3 networks) colored solids.

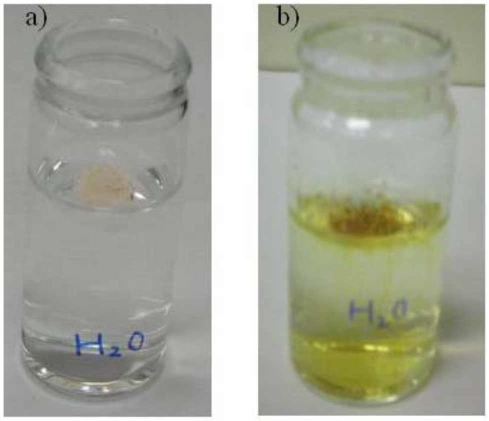

Figure 3. 1. Silica networks synthesized using a) G3 dendrimer and b) G4 dendrimer in aqueous silver acetate solution.

Generation 4 dendrimer templated silica network initially floated on the surface of aqueous silver acetate solution, however, upon stirring, it started to wet with the solution (Figure 3.1b). The color of the network changed quickly to green upon mixing and an intense smell of acetic acid was noted, indicating grafting of silver ions. After stirring for about an hour, the solvent was slowly removed on a rotary evaporator at 40 ˚C. The residue was rinsed with water, filtered under vacuum, yielding a dark solid.

Characterization of the resulting solids was carried out using a combination of techniques including UV-Vis spectroscopy, X-ray powder diffraction (XRPD) and transmission electron microscopy (TEM). The UV-Vis spectra of metal particles synthesized using G1-3 dendrimer templated networks, showed peaks at 413, 431, 427 nm respectively, and for those from G4 templated network showed absorption at 461 nm (Figure 3.2). The variations in the particle resonance absorption peaks are associated with the size of the nanoparticles, and an increase in resonance absorption is indicative of increased particle size in these assemblies [8].

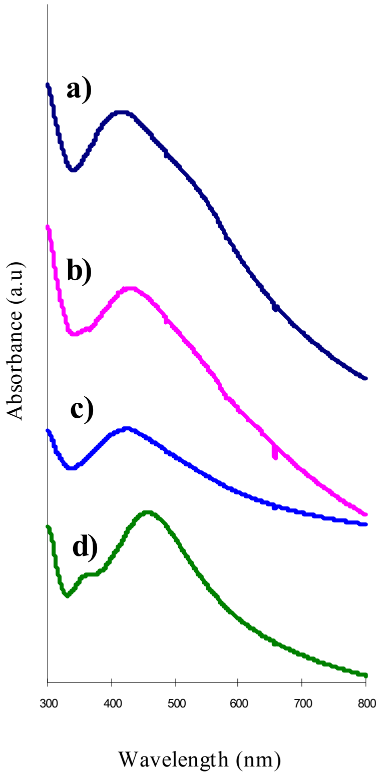

Figure 3. 2. UV-Vis absorption spectra of silver particles synthesized using G1 (a), G2 (b), G3 (c) and G4 (d) dendrimer templated networks.

X-ray powder diffraction analyses (XRPD) of the silver particles constructed from G1-3 networks showed strong 2θ (^{o}) peaks at 32.30, 46.45, 55.0, 57.7 which can be assigned to the Ag_2O phase [6] of particles present in these networks (Figure 3.3A). For the metal particles constructed using G4 templated network, no silver oxide phase was detected, and it showed peaks at 2θ (^{o}) 38.25 (111), 44.60 (200), 64.90 (220) and 77.65 (311), corresponding to the *fcc* silver metal particles (Figure 3.3B).

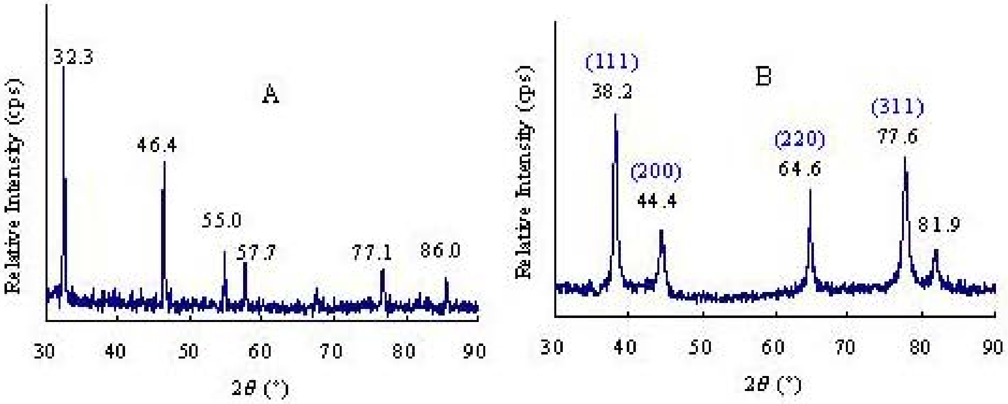

Figure 3. 3. XRPD analysis of nanoparticles synthesized using G1 (A) and G4 (B) dendrimer templated networks.

Transmission electron microscopy (TEM) analyses of the nanoparticles showed that these are distributed inside the networks. Figures 3.4 and 3.5 (left) below show the TEM images of metal particles constructed using G1-3 dendrimer templated networks, and a globular morphology of the particles is generally observed. The particle sizes ranged between 10-50 nm with an average size of ~25 nm. In general, there was an increase in the average particle size in going from G1-3 networks. This is consistent with the pore size increase in these networks [5], and as expected, an increase in the internal space in these pores, leads to an increase in the size of the nanoparticles.

TEM image of silver particles synthesized using G4 dendrimer templated network is shown in Figure 3.5 (right). The size range of these particles was between 25-80 nm, with an average size of ~45 nm, which is higher than the size of the particles obtained from G1-3 templated silica networks, and is in line with the increased pore size in this network [5].

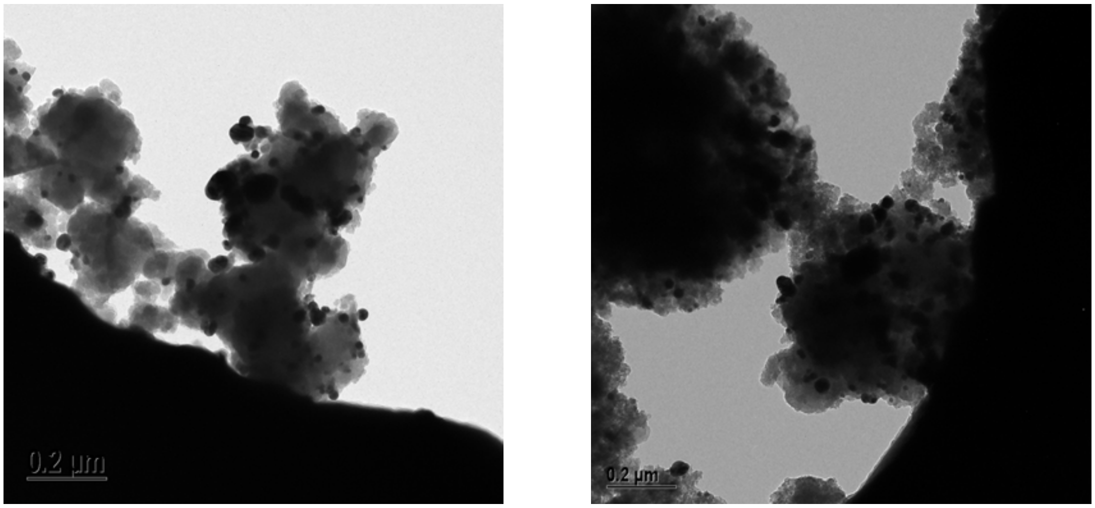

Figure 3. 4. TEM images of nanoparticles synthesized using generation 1 (left) and 2 (right) dendrimer templated silica networks.

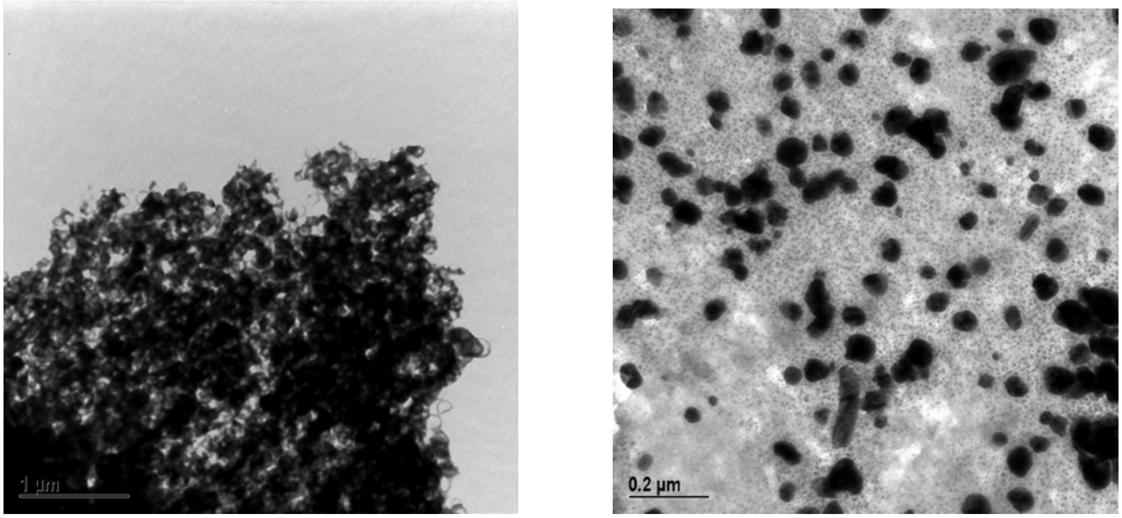

Figure 3. 5. TEM image of nanoparticles synthesized using generation 3 (left) and 4 (right) dendrimer templated silica networks.

It is well known that silver acetate reacts with acidic groups including silanol (Si-OH), leading to the formation of acetic acid and grafted silver ions [3, 7]. An evaluation of the nanoparticle syntheses in G1-4 dendrimer templated silica networks is detailed in Scheme 3.1.

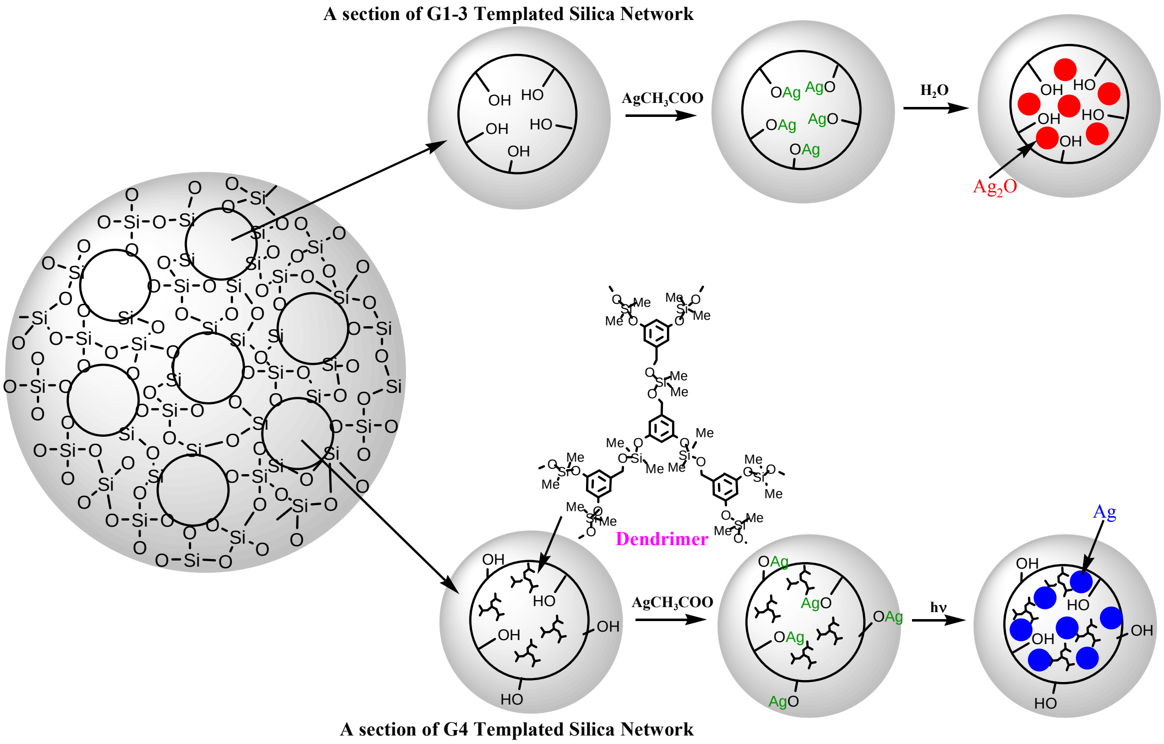

Scheme 3. 1. The evaluation of the nanoparticle syntheses in G1-4 dendrimer templated silica networks.

Since G1-3 silica networks do not mix with water and float on its surface (Figure 3.1a), there is very slow inclusion of aqueous silver acetate into the network. Silver acetate then reacts with silanol groups and silver ions are slowly chemisorbed into the interior of the network. The wet interior atmosphere with increased local water content around the metal ions, then promotes the formation of Ag_2O particles. The reduction of silver ions photolytically could be a competitive process, leading to the formation of silver metal particles. However, due to lack of any stabilizing environment, it will be much slower than the silver oxide nanoparticle build-up.

G4 network contains dendrimer template in it, which was confirmed by solid-state $^{13}C\{^1H\}$ NMR (Figure 3.6) that showed peaks related to the 3,5-dihydroxybenzyl alcohol backbone linked by Me_2Si groups. It mixes with silver acetate solution upon stirring (Figure 3.1b), which can be explained by considering that some of the Si-OH groups point outwards in this network because of their unfavorable interactions with dendrimers. Upon mixing, silver ions get chemisorbed (Scheme 3.1), as described above, and due to a stabilizing environment presented by the dendrimer in G4 network, these get reduced to silver metal particles photolytically. The formation of silver oxide is excluded in this network, since reduction under stabilizing environment of phenyl groups of the dendrimer, is much faster and is favored over the formation of silver oxide. It is interesting to note that if the dendrimer template is completely removed from the G4 dendrimer templated network, then silver oxide formation, similar to that described above for G1-3 dendrimer templated networks, is observed.

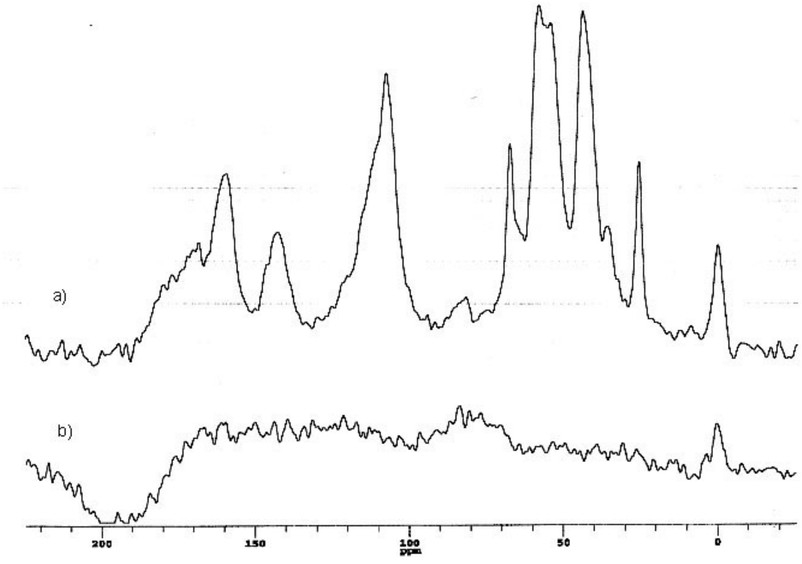

Figure 3. 6. Solid-sate $^{13}C\{^{1}H\}$ NMR spectra of a) G4 dendrimer templated silica network, and b) G3 dendrimer templated silica network.

3.2.4. Conclusion

Silica networks constructed using dendrimers as templates are ideal candidates in designing a simple methodology to synthesize silver or silver oxide nanoparticles. Networks from which 3,5-dihydroxy benzyl alcohol based dendrimer templates are effectively and completely removed, do not mix with silver acetate solution. Slow inclusion of aqueous silver acetate into these networks leads to chemisorption of silver ions in their interior. Due to increased water content locally, it is followed by the formation of silver oxide nanoparticles. In contrast, network that contains residual dendrimer template, mixes with silver acetate solution easily, and silver ions get grafted upon mixing with silver acetate solution. Photolytic reduction under a stabilizing dendrimer environment follows, leading to the formation of silver metal particles exclusively. Thus, dendrimer templated networks with variable internal environments, offer the desired potential in tailoring the synthesis of silver nanoparticles.

3.2.5 Acknowledgments

We would like to thank NSERC of Canada and McGill Center for Self-Assembled Chemical Structures (FQRNT, Quebec, Canada) for financial assistance.

References

1. (a) Hu M, Chen J, Li Z-Y, Au L, Hartland G V, Li X, Marquez M and Xia Y 2006 *Chem. Soc. Rev.* **35** 1084. (b) Daniel M-C and Astruc D 2004 *Chem. Rev.* **104** 293. (c) Stankic S, Sterrer M, Hofmann P, Bernardi J, Diwald O and Knozinger E 2005 *Nano Lett.* **5** 1889. (d) Huang C-C Chang and H-T 2006 *Anal. Chem.* **78** 8332. (e) Zheng N and Stucky G D 2006 *J. Am. Chem. Soc.* **128** 14278. (f) Choi J-S, Jun Y-W, Yeon S-I, Kim H C, Shin J-S and Cheon J 2006 *J. Am. Chem. Soc.* **128** 15982.
2. (a) Sun Y and Xia Y 2002 *Science* **298** 2176. (b) Whelan A M, Brennan M E, Blau W J and Kelly J M 2004 *J. Nanosci. Nanotechnol.* **4** 66. (c) Watanabe K, Menzel D, Nilius N and Freund H-J 2006 *Chem. Rev.* **106** 4301. (d) Bell S E J and Sirimuthu N M S 2006 *J. Am. Chem. Soc.* **128** 15580. (e) Gu X, Nie C, Lai Y and Lin C 2006 *Mater. Chem. Phys.* **96** 217. (f) Ledwith D M, Whelan A M and Kelly J M 2007 *J. Mater. Chem.* **17** 2459.
3. (a) Armelao L, Bottaro G, Campostrini R, Gialanella S, Ischia M, Poli F and Tondello E 2007 Nanotechnology **18** 155606. (b) Gacoin T, Besson S and Boilot J P 2006 *J. Phys.: Condens. Matter* **18** S85–S95.
4. (a) Petrucci M G L, Guillemette V, Dasgupta M and Kakkar A K 1999 *J. Am. Chem. Soc.* **121** 1968. (b) Dasgupta M, Peori B and Kakkar A K 2002 *Coord. Chem. Rev.* **223** 233. (c) Bourrier O and Kakkar AK 2003 *J. Mater. Chem***.** **13** 1306. (d) Bourrier O, Butlin J, Hourani R and Kakkar A K 2004 *Inorg. Chim. Acta* **357** 3836. (e) Hourani R, Whitehead M A and Kakkar A K 2005 *J. Mater. Chem.* **15** 2106.
5. Czerniewski A A, Liu X J, Rolland O, Hourani R, Four M, Kakkar A K 2007 *J. Mater. Chem.* **17** 2737.
6. (a) Shchukin D M, Radtchenko I L, Sukhorukov G B 2003 *CHEMPHYSCHEM* **4** 1101. (b) Waterhouse G I N, Bowmaker G A, Metson J B 2002 *Surf. Interface Anal.* **33** 401.
7. (a) Belli dell’Amico D, Lora S, D’Archivio AA, Galantini L, Biffis A and Corain B 2000, *J. Mol. Catal. A* **157** 173. (b) Corain B, Scanagatta E, Basato M, Valle G, Sitran S and Veronese AC 1988 *Inorg. Chim. Acta* **148** 105.

8. Chiu Y, Rambabu U, Hsu M-H, Shieh H-P D, Chen C-Y, Lin H-H, 2003, *J. Appl. Phys*. **94** *(3)* 1996.

Chapter 4: Conclusions and Suggestions for Future Work

4.1. Conclusions

This thesis reports construction of dendrimer templated silica networks using a simple sol-gel condensation methodology. 3,5-dihydroxybenzyl alcohol (DHBA) based dendrimers of generations 0 to 5 were used as templates to prepare a variety of organic-inorganic hybrid networks from which organic moieties are removed *in situ* or upon acid hydrolysis. The detailed studies of silica network structures and surface morphology were carried out using techniques including FT-IR, solid state ^{29}Si and ^{13}C{^{1}H} NMR, transmission electron microscopy (TEM), and surface area analysis (BET). These dendrimer templated silica networks were subsequently employed in tailoring the synthesis of silver metal nanoparticals. Their sizes and shapes depend on the internal environment of silica networks.

4.1.1 Construction of silica networks using 3,5-dihydroxybenzylalcohol (DHBA) based dendrimers as templates

The goal of this thesis was to synthesize porous and highly cross-linked silica based networks by using DHBA based dendrimers of generations 1 to 5 as templates, and two types of silane reagents. The DHBA based dendrimers contain corresponding peripheral hydroxyl groups, which help generate dendrimer aggregates in solution through hydrogen bonding, a commonly observed phenomenon that occurs for these types of dendrimers. These aggregated dendrimers were then employed as templates in the preparation of silica networks, in which the dendrimer generation and its ability to aggregate strongly influence the morphology of the resulting silica networks. The detailed analysis of silica networks using a combination of techniques, including FT-IR, TEM, and solid-state ^{29}Si and ^{13}C{^{1}H} NMR, clearly shows the crucial role of aggregation in the polycondensation process that leads to silica network formation around these aggregates and subsequently determines their internal structure. Dendrimers of generation 1-3 provide a slightly better control on the evolving structure of the silica networks, due to the smaller size of dendritic aggregates compared to those of generation 4-5. In addition, choice of the silane reagent also plays an important role in the evolution of silica network. In this synthesis, aminosilane reagents that were employed in the sol-gel process included tetrakis(dimethylamino)silane [$Si(NMe_2)_4$] and chlorotris(diethylamino)silane [$ClSi(NEt_2)_3$]. $ClSi(NEt_2)_3$ provides a one-pot synthesis, while the $Si(NMe_2)_4$ yields silica networks with much higher surface area. The pore sizes in generation 1-5 templated networks prepared using $Si(NMe_2)_4$, were found to increase with the dendrimer generation, It has been demonstrated that larger the dendrimer generation, larger the dendrimer aggregates.

The removal of dendritic moieties was carried out *in situ* or upon acid hydrolysis. The former reaction relates to a one-pot synthesis using $ClSi(NEt_2)_3$ as the coupling silane reagent that produces hydrochloric acid as a by-product, helps remove the dendrimer templates from the silica networks *via* acid hydrolysis. Diethylammoniumchloride salt (a by-product formed during the reaction) gets trapped inside the silica network, the removal of which leads to significant enhancement of surface area. Removal of dendrimer templates and salt was confirmed by solid-state $^{13}C\{^{1}H\}$ NMR spectroscopy, in which silica networks prepared using generations 1-3 dendrimer templates show complete removal of the dendritic moieties and salt (no peaks in the $^{13}C\{^{1}H\}$ NMR spectroscopy), while there is still salt left in those prepared from generation 4-5 dendrimer templates. This is due to a relative large quantity of salt produced in the polycondensation process when generation 4-5 dendrimers are used as templates, and rinsing with water does not remove the salt completely. When $Si(NMe_2)_4$ is used as the coupling reagent, the residual dendritic moieties are still present as indicated by the $^{13}C\{^{1}H\}$ NMR spectra of silica networks synthesized using generation 4-5 dendrimer as templates. The acid hydrolysis does not remove the latter dendritic templates completely from silica networks, due to denser globular dendritic aggregates that are formed through a large amount of hydrogen bonds.

The surface of these silica networks was found to be hydrophobic with a hydrophilic interior. The potential application of these networks in small molecule encapsulation was demonstrated by disperse red 1 (DR1) entrapment in these silica networks using sonication.

4.1.2 Silver nanoparticle assemblies using dendrimer templated silica networks

In this thesis one of the potential applications of silica networks synthesized using DHBA based dendrimer templates was explored in constructing silver oxide or silver metal nanoparticles. Silica networks prepared using generation 0-4 dendrimer templates were employed successfully in tailoring the synthesis of silver nanoparticles. Slow inclusion of aqueous silver acetate into silica networks leads to chemisorption of silver ions into the interior of the networks. Due to increased local water content around the metal ions, it is followed by the formation of silver oxide nanoparticles. The characterization by X-ray podwer diffraction (XRPD) showed that the particles were mainly silver oxide in G0-networks. From G1 to G3-networks silver metal nanoparticles were also formed, due to a competitive process of photolytic reducation. Transmission electron microscopy (TEM) analysis of the nanoparticles showed that metal particles constructed using G1-3 networks are of globular morphology with the size range between 10-50 nm with an average of ~25 nm. The average particle size increased from G0 to G3 due to the pore size increase in these silica networks.

Due to residual dendrimer templates inside silica networks constructed using G 4 dendrimer templated silica network, it is easy to wet with silver acetate solution after stirring. The color changed quickly to green with intense smell of acetic acid indicating the grafting of silver ions. Silver ions were then reduced to silver metal particles photolytically in the stabilizing environment of residual dendrimer templates in silica networks.

4.2 Future Outlook

Constructing porous materials with tailored internal environment continues to be a topical area of research. Dendrimer templated silica networks have offered a good platform to construct such materials. It will be interesting to carry out more detailed analysis of these silica networks to obtain structure-property relationships related to pore size, using a combination of techniques including nitrogen desorption isotherm method and TEM. The advantage of removal of dendrimer templates from silica networks by *in situ* or acid hydrolysis could be comparied with those silica networks in which dendrimer templates are removed by calcinations. The thermal analysis such as DSC and TGA of silica networks could also be further explored. These studies will strengthen their significance in applications in sorption and molecular encapsulation.

The surface of these silica networks is hydrophobic with a hydrophilic interior. It would be interesting to take advantage of this behavior and investigate encapsulation and controlled release of small molecules from silica networks.

Construction of silver oxide and silver metal nanoparticles inside these networks has offered intriguing opportunities in designing novel materials. It would be interesting to fully understand silver metal nanoparticle formation inside G4-networks with residual dendrimer templates. It will be interesting to make a variety of such networks with and without dendrimer templates and investigate the formation of metal and metal oxide nanoparticles.

Finally, these silica networks could also be used to include other metal particles such as gold or copper. The study of their structure-property relationships could then be compared to those of silver metal nanoparticles, and used to develop metal nanoparticle based devices.